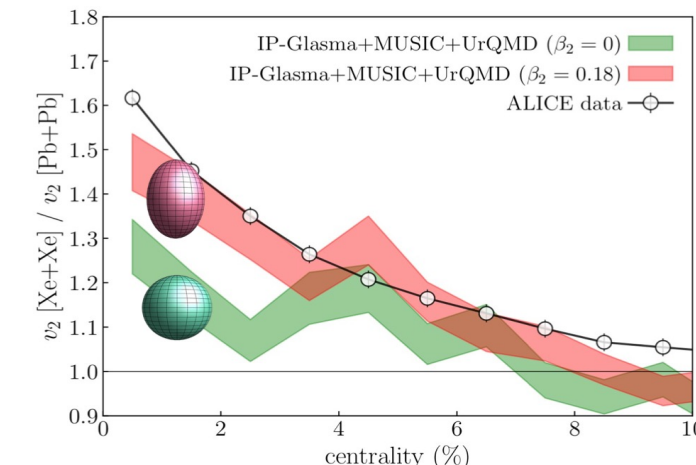
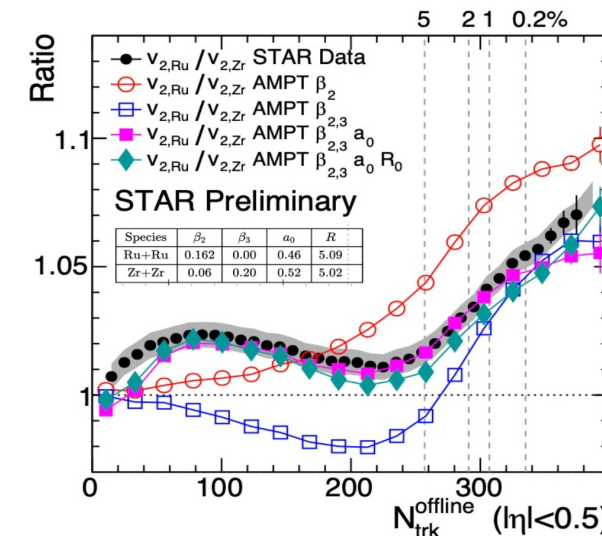
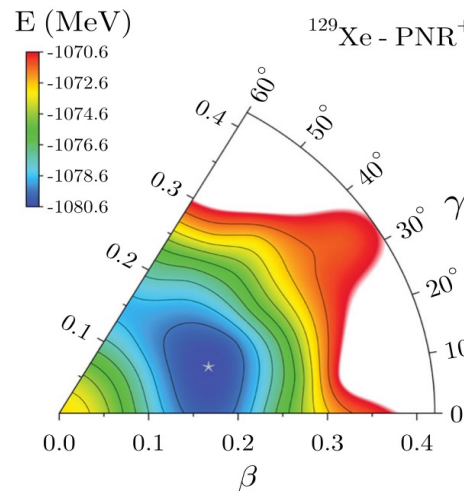


Energy dependence of initial condition from isobar

Based on: 2301.01294



MeV

200 GeV

5 TeV

Introduction

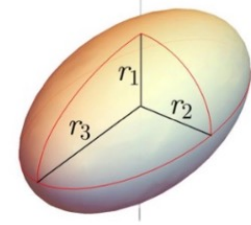
- Nuclear deformation parameters are generally estimated from spectroscopic methods:

$$\rho(r) = \frac{\rho_0}{[1 + \exp(r - R(\theta, \phi))/a]}$$

Nuclear geometry: Woods-Saxon

$$R(\theta, \phi) = R_0(1 + \beta(\cos\gamma Y_{20}(\theta, \phi) + \sin\gamma Y_{22}(\theta, \phi)))$$

Parametrization of deformation



$$\beta = \frac{4\pi}{3ZeR_0^2} \sqrt{B(E2) \uparrow}$$

Estimation of deformation

Introduction

- Nuclear deformation parameters are generally estimated from spectroscopic methods:

$$\rho(r) = \frac{\rho_0}{[1 + \exp(r - R(\theta, \phi))/a]}$$

Nuclear geometry: Woods-Saxon

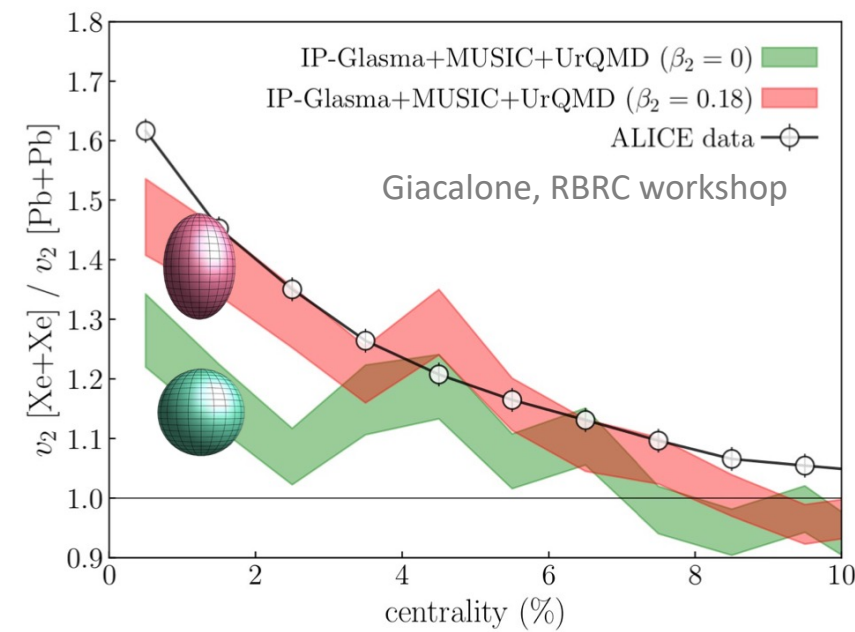
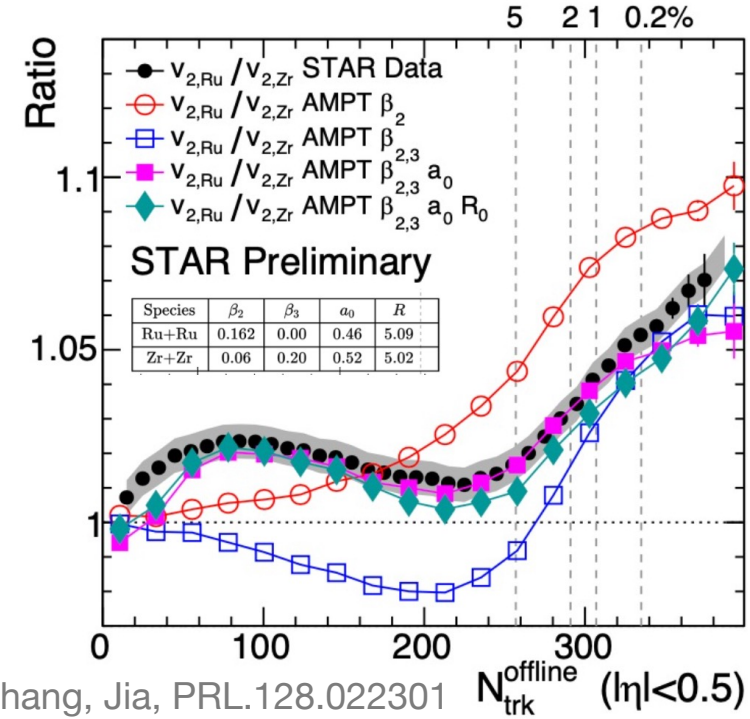
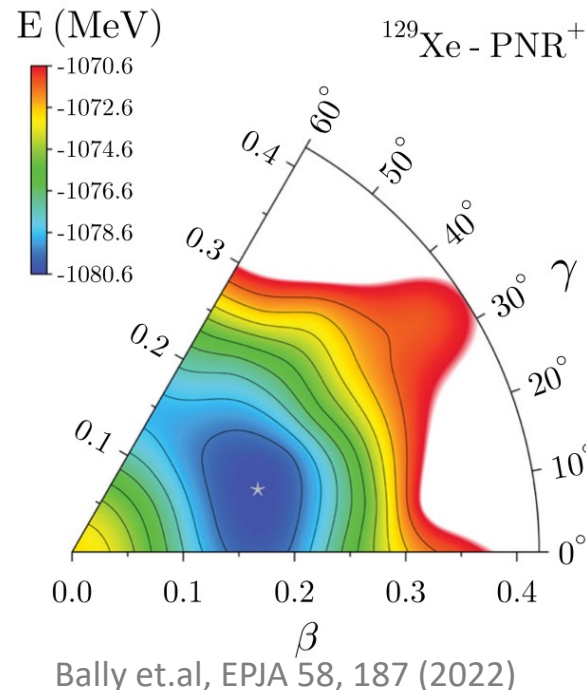
$$R(\theta, \phi) = R_0(1 + \beta(\cos\gamma Y_{20}(\theta, \phi) + \sin\gamma Y_{22}(\theta, \phi)))$$

Parametrization of deformation

$$\beta = \frac{4\pi}{3ZeR_0^2} \sqrt{B(E2) \uparrow}$$

Estimation of deformation

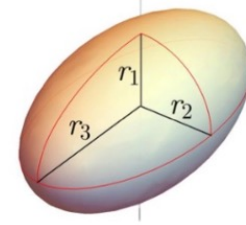
- Clear impact of nuclear structure on final state heavy-ion observables: N_{ch} , $v_{2,3}$, $[p_T]$ and $\rho(v_2^2, [p_T])$



MeV

200 GeV

5 TeV



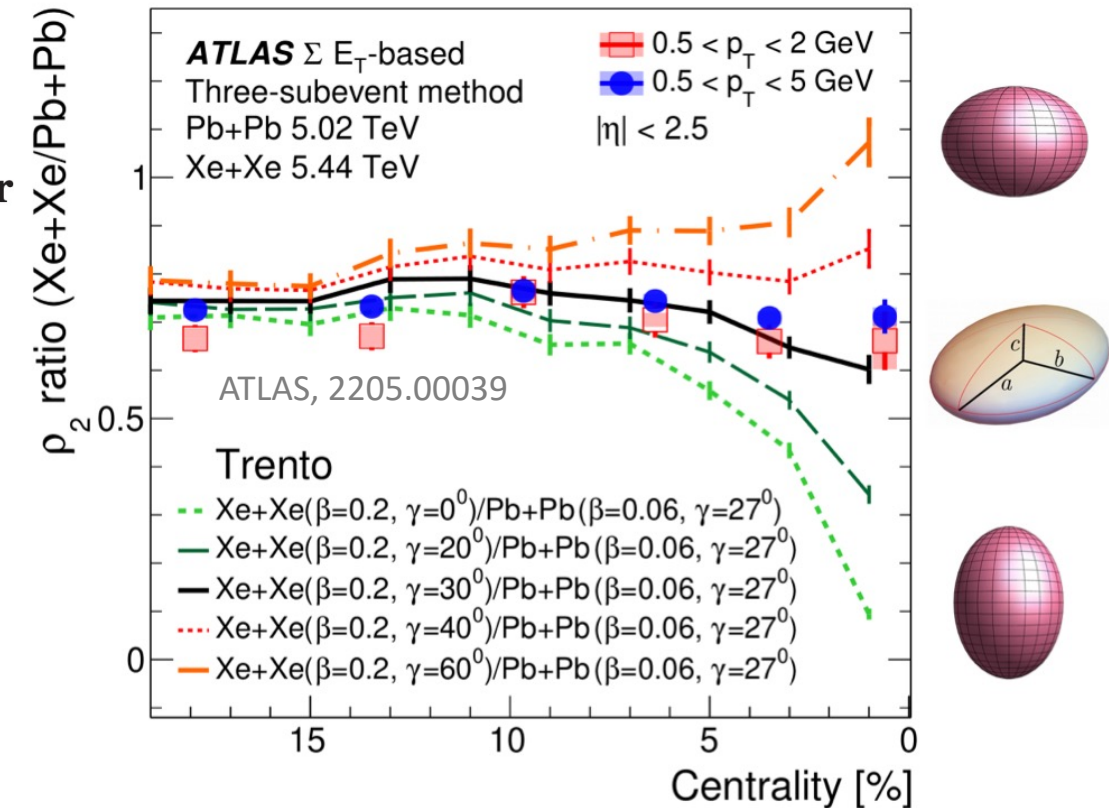
Open Question: Does nuclear deformation change with energy scales?

PHYSICAL REVIEW LETTERS 128, 082301 (2022)

Evidence of the Triaxial Structure of ^{129}Xe at the Large Hadron Collider

Benjamin Bally¹, Michael Bender², Giuliano Giacalone³, and Vittorio Somà⁴

- Few indications of consistent descriptions between Low energy predictions and observations at LHC energy.



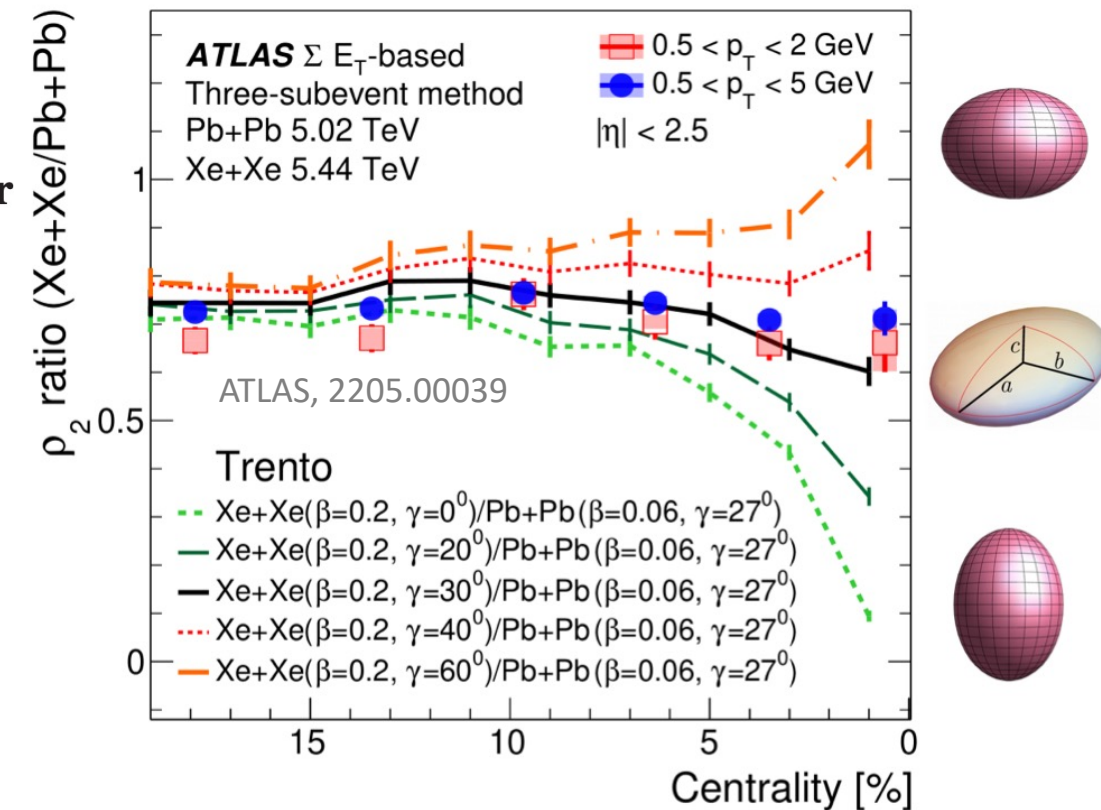
Open Question: Does nuclear deformation change with energy scales?

PHYSICAL REVIEW LETTERS 128, 082301 (2022)

Evidence of the Triaxial Structure of ^{129}Xe at the Large Hadron Collider

Benjamin Bally¹, Michael Bender², Giuliano Giacalone³, and Vittorio Somà⁴

- Few indications of consistent descriptions between Low energy predictions and observations at LHC energy.



- ❖ To answer this question, we simulate Heavy ion collisions at 200 GeV and 5 TeV for Ru+Ru and Zr+Zr to study the effect of deformation across these energy scales.

Goal of this study and Model used

Goal: Check consistency of effect of nuclear deformation between 200 GeV and 5 TeV using isobar collisions.

Model Used:

- AMPT (String Melting) model: Multiple stages for evolution.
- Transport framework, Good proxy for hydro simulation.

- Model Parameters used:

| Model params | Lund's a | Lund's b | hadron cascade time | Events/case |
|--------------|----------|----------|---------------------|-------------|
| 200 GeV | 0.55 | 0.15 | 15 fm | 200 mil |
| 5 TeV | 0.30 | 0.15 | 60 fm | 12 mil |

- Systems under consideration:

| Cases | β_2 | β_3 | a_0 | R |
|-----------|-----------|-----------|-------|------|
| Ru (def.) | 0.162 | 0 | 0.46 | 5.09 |
| Case 2 | 0.06 | 0 | 0.46 | 5.09 |
| Case 3 | 0.06 | 0.2 | 0.46 | 5.09 |
| Case 4 | 0.06 | 0.2 | 0.52 | 5.09 |
| Zr | 0.06 | 0.2 | 0.52 | 5.02 |

Goal of this study and Model used

Goal: Check consistency of effect of nuclear deformation between 200 GeV and 5 TeV using isobar collisions.

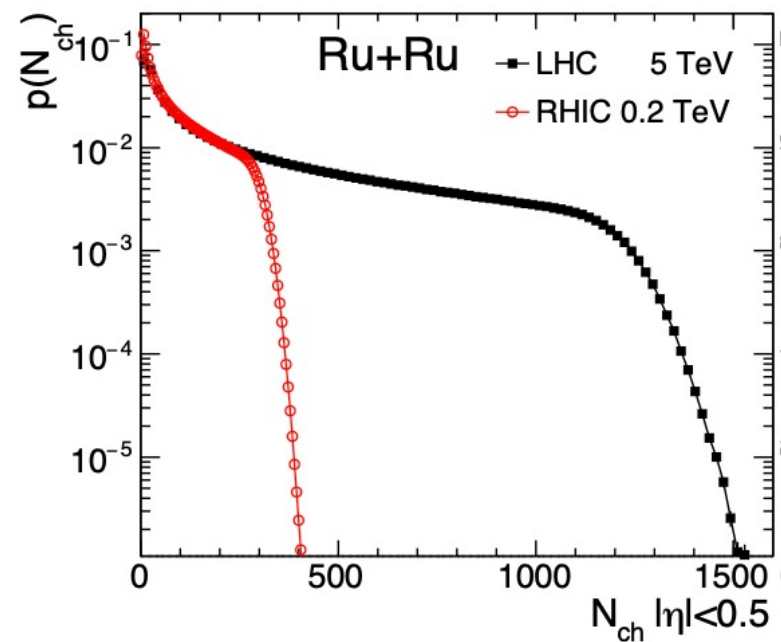
Model Used:

- AMPT (String Melting) model: Multiple stages for evolution.
- Transport framework, Good proxy for hydro simulation.
- Model Parameters used:

| Model params | Lund's a | Lund's b | hadron cascade time | Events/case |
|--------------|----------|----------|---------------------|-------------|
| 200 GeV | 0.55 | 0.15 | 15 fm | 200 mil |
| 5 TeV | 0.30 | 0.15 | 60 fm | 12 mil |

- Systems under consideration:

| Cases | β_2 | β_3 | a_0 | R |
|-----------|-----------|-----------|-------|------|
| Ru (def.) | 0.162 | 0 | 0.46 | 5.09 |
| Case 2 | 0.06 | 0 | 0.46 | 5.09 |
| Case 3 | 0.06 | 0.2 | 0.46 | 5.09 |
| Case 4 | 0.06 | 0.2 | 0.52 | 5.09 |
| Zr | 0.06 | 0.2 | 0.52 | 5.02 |



Goal of this study and Model used

Goal: Check consistency of effect of nuclear deformation between 200 GeV and 5 TeV using isobar collisions.

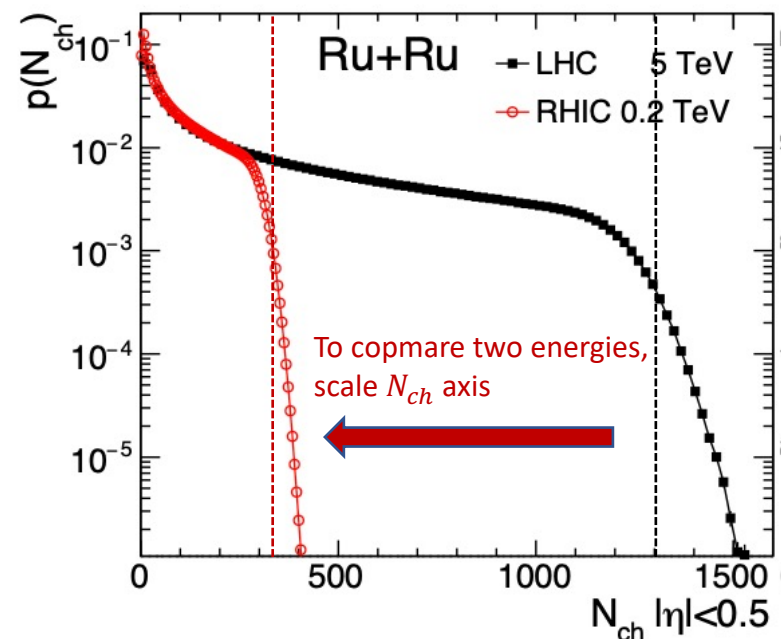
Model Used:

- AMPT (String Melting) model: Multiple stages for evolution.
- Transport framework, Good proxy for hydro simulation.
- Model Parameters used:

| Model params | Lund's a | Lund's b | hadron cascade time | Events/case |
|--------------|----------|----------|---------------------|-------------|
| 200 GeV | 0.55 | 0.15 | 15 fm | 200 mil |
| 5 TeV | 0.30 | 0.15 | 60 fm | 12 mil |

- Systems under consideration:

| Cases | β_2 | β_3 | a_0 | R |
|-----------|-----------|-----------|-------|------|
| Ru (def.) | 0.162 | 0 | 0.46 | 5.09 |
| Case 2 | 0.06 | 0 | 0.46 | 5.09 |
| Case 3 | 0.06 | 0.2 | 0.46 | 5.09 |
| Case 4 | 0.06 | 0.2 | 0.52 | 5.09 |
| Zr | 0.06 | 0.2 | 0.52 | 5.02 |



Goal of this study and Model used

Goal: Check consistency of effect of nuclear deformation between 200 GeV and 5 TeV using isobar collisions.

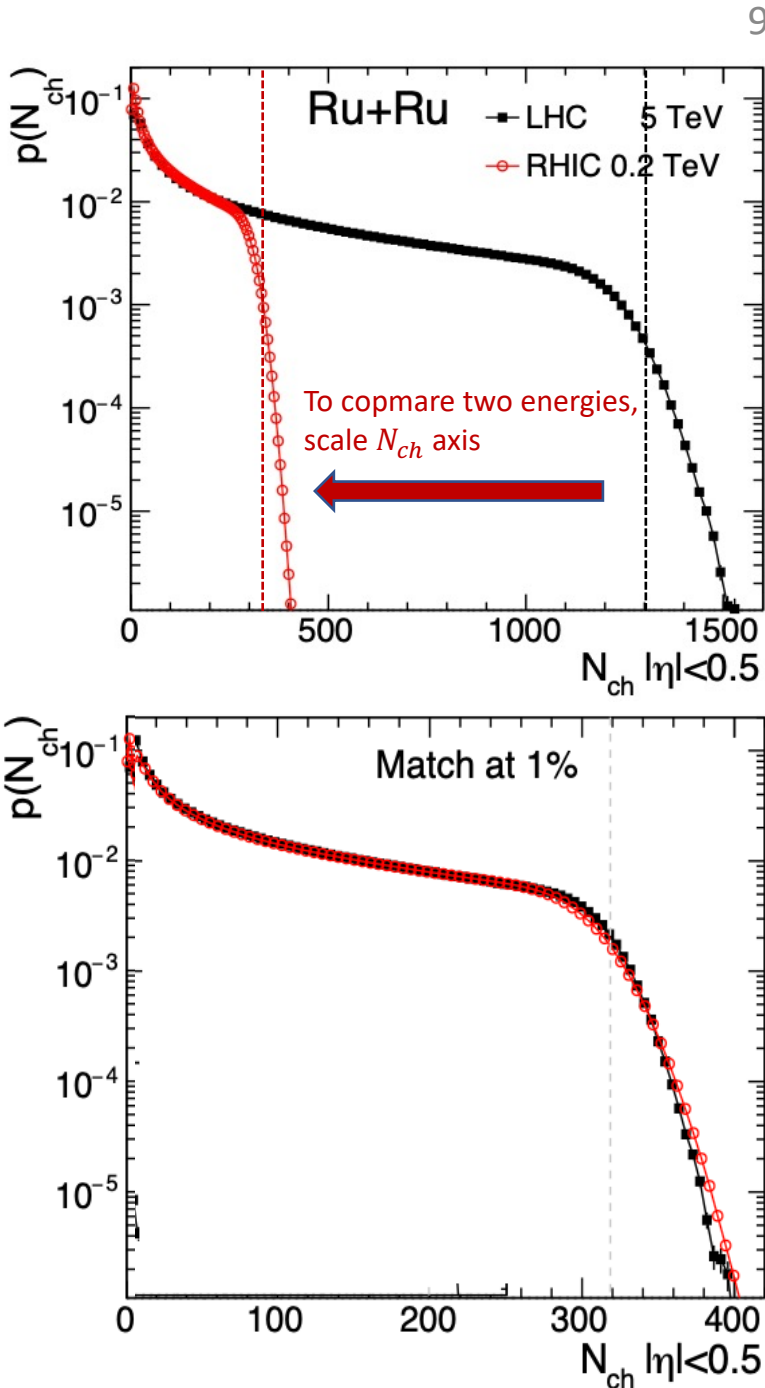
Model Used:

- AMPT (String Melting) model: Multiple stages for evolution.
- Transport framework, Good proxy for hydro simulation.
- Model Parameters used:

| Model params | Lund's a | Lund's b | hadron cascade time | Events/case |
|--------------|----------|----------|---------------------|-------------|
| 200 GeV | 0.55 | 0.15 | 15 fm | 200 mil |
| 5 TeV | 0.30 | 0.15 | 60 fm | 12 mil |

- Systems under consideration:

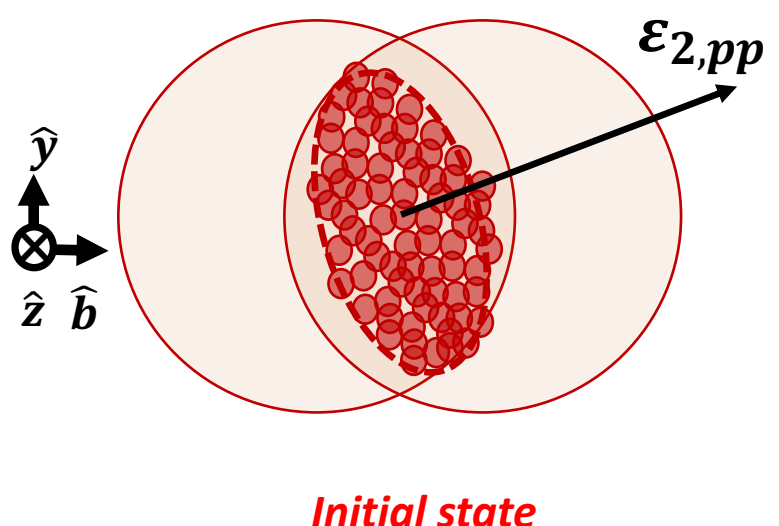
| Cases | β_2 | β_3 | a_0 | R |
|-----------|-----------|-----------|-------|------|
| Ru (def.) | 0.162 | 0 | 0.46 | 5.09 |
| Case 2 | 0.06 | 0 | 0.46 | 5.09 |
| Case 3 | 0.06 | 0.2 | 0.46 | 5.09 |
| Case 4 | 0.06 | 0.2 | 0.52 | 5.09 |
| Zr | 0.06 | 0.2 | 0.52 | 5.02 |



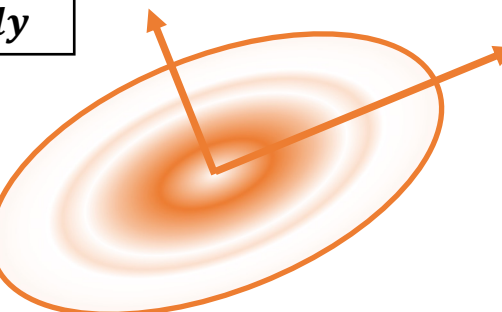
PART I:

Impact of fluctuations on Flow ratios in isobar collisions.

Final state Elliptic Flow (v_2)

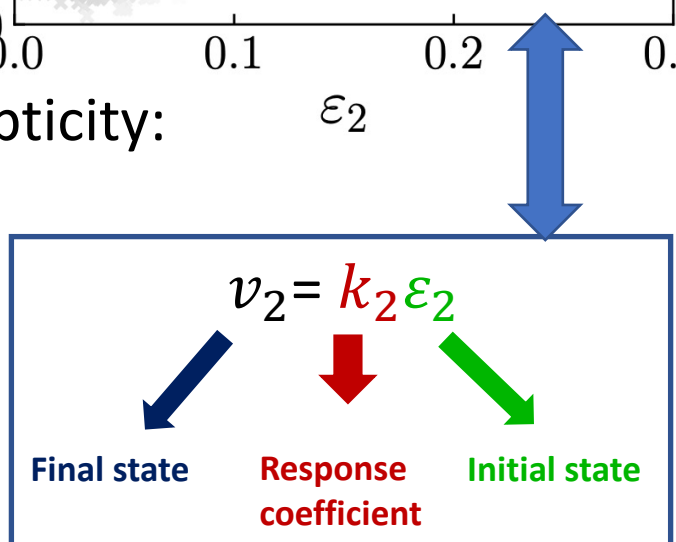
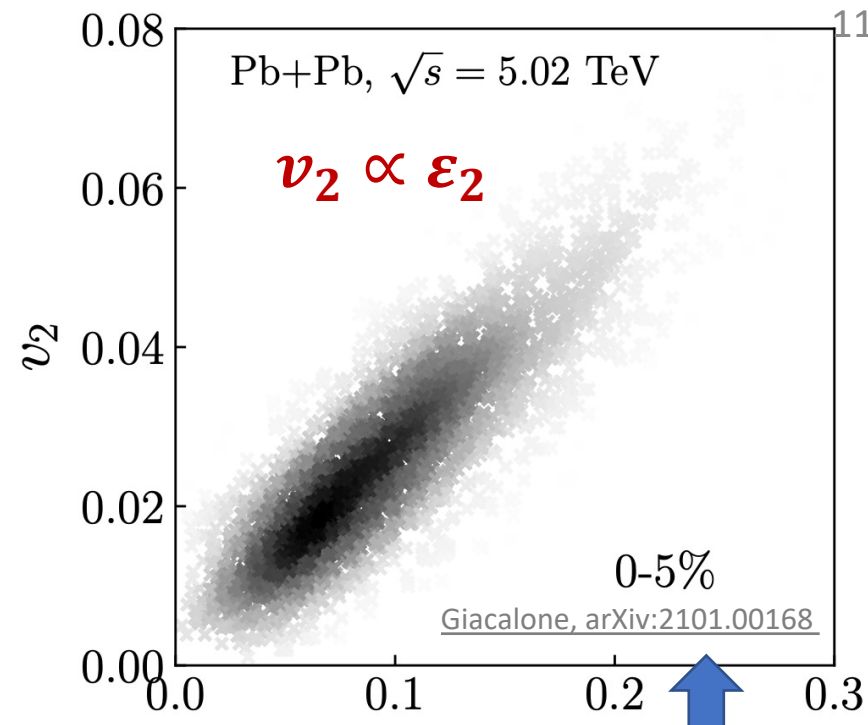


$$\frac{dP}{dx} > \frac{dP}{dy}$$

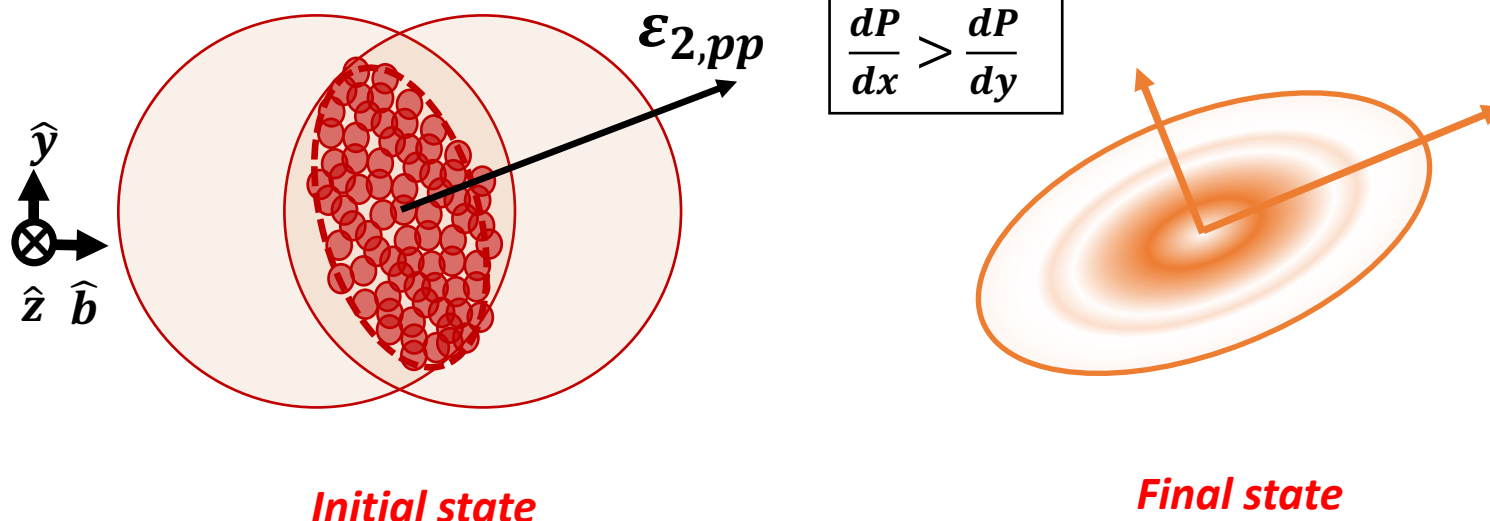


Final state

- Flow develops as a pressure gradient driven response to initial ellipticity:

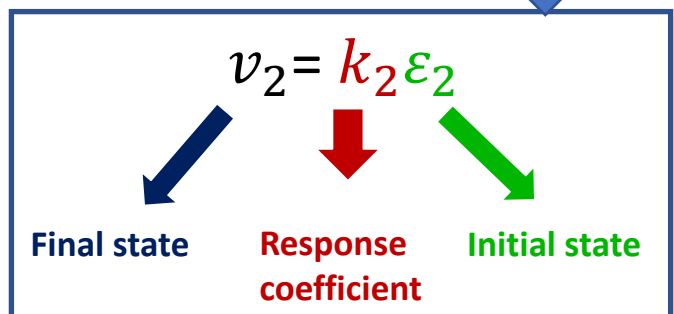
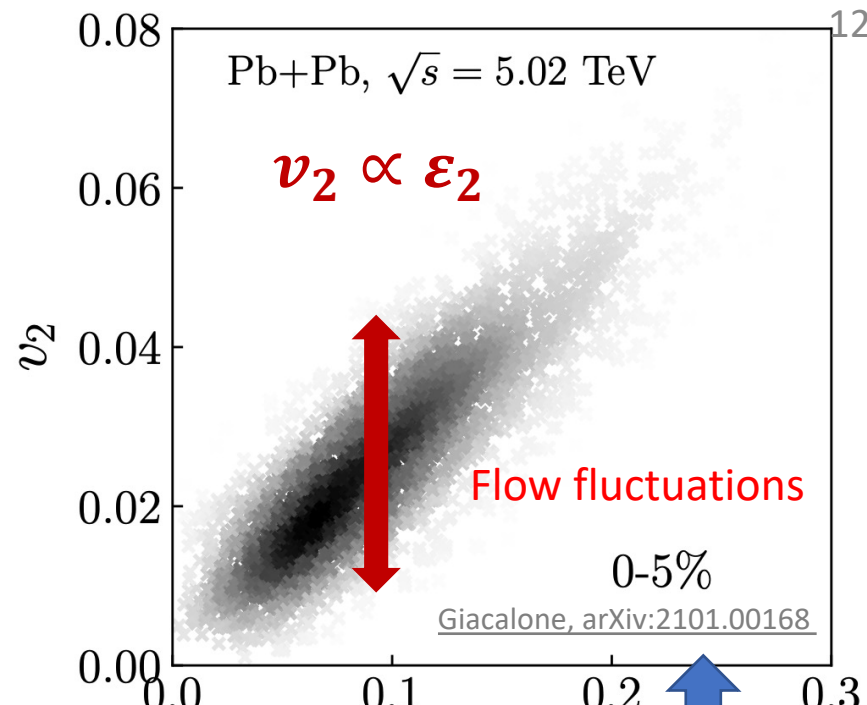


Final state Elliptic Flow (v_2)

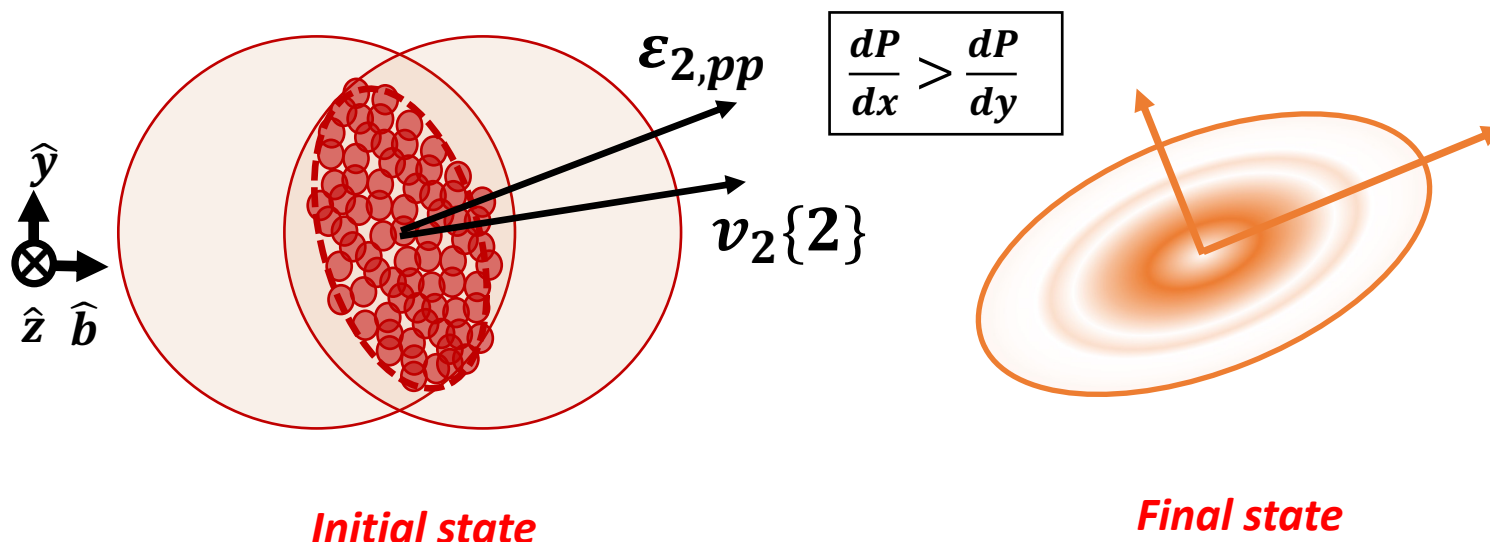


$$\frac{dP}{dx} > \frac{dP}{dy}$$

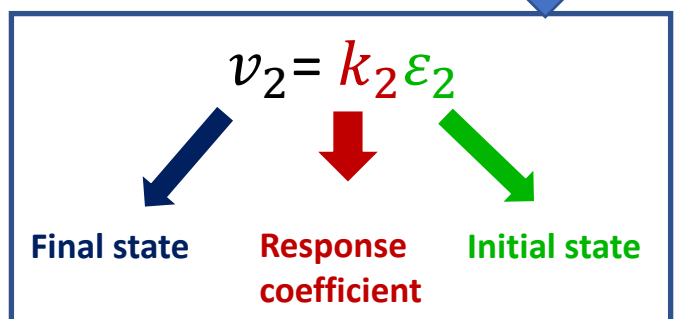
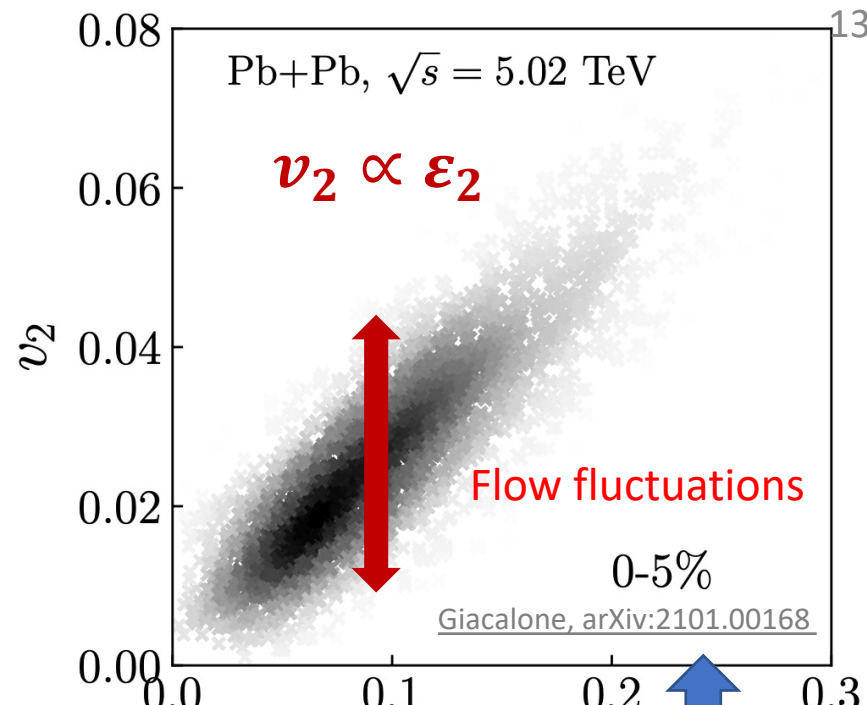
- Flow develops as a pressure gradient driven response to initial ellipticity:
- But the proportionality: $v_2 \propto \varepsilon_2$ is true only on an average.



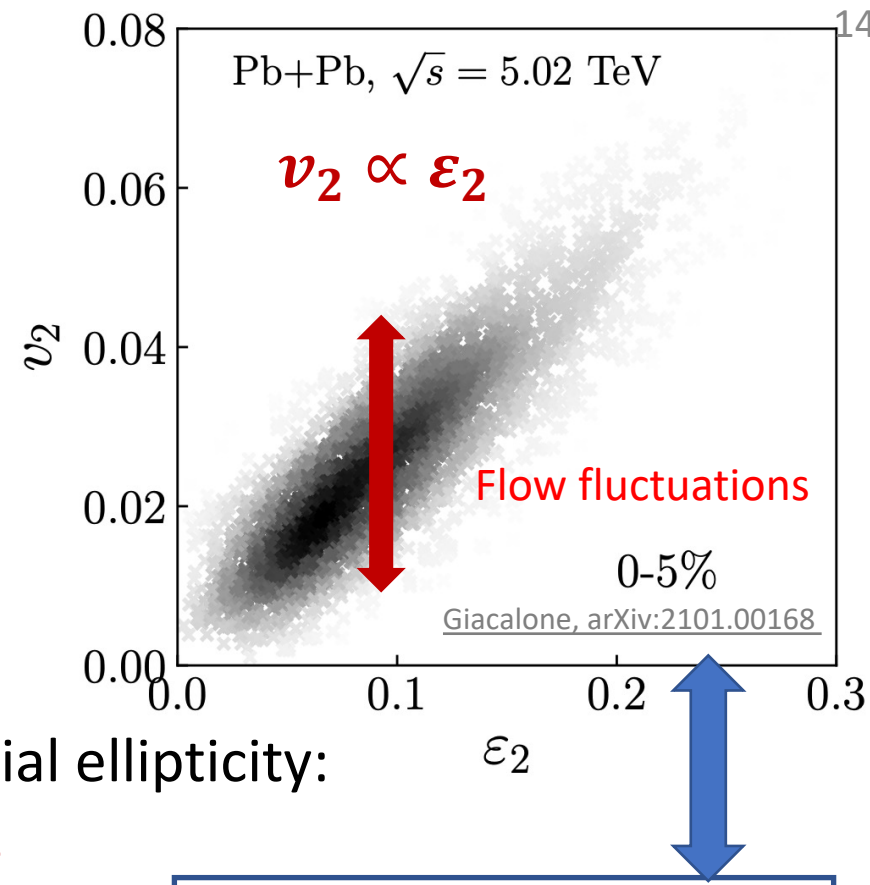
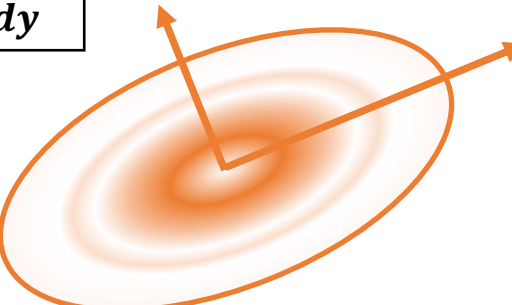
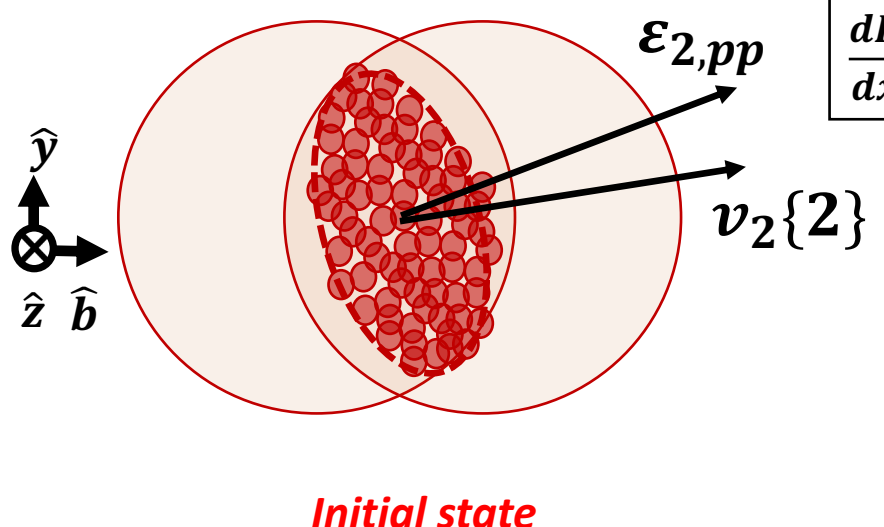
Final state Elliptic Flow (v_2)



- Flow develops as a pressure gradient driven response to initial ellipticity:
- But the proportionality: $v_2 \propto \varepsilon_2$ is true only on an average.
- In reality, the measured $v_2\{2\}$: $v_2^2\{2\} = v_{2,pp}^2 + \delta_2^2$



Final state Elliptic Flow (v_2)

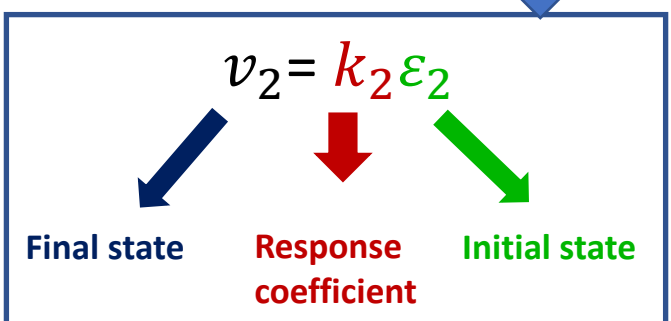


- Flow develops as a pressure gradient driven response to initial ellipticity:
- But the proportionality: $v_2 \propto \epsilon_2$ is true only on an average.
- In reality, the measured $v_2\{2\}$: $v_2^2\{2\} = v_{2,pp}^2 + \delta_2^2$

Flow originating from participant geometry.

Part of flow uncorrelated to participant geometry.

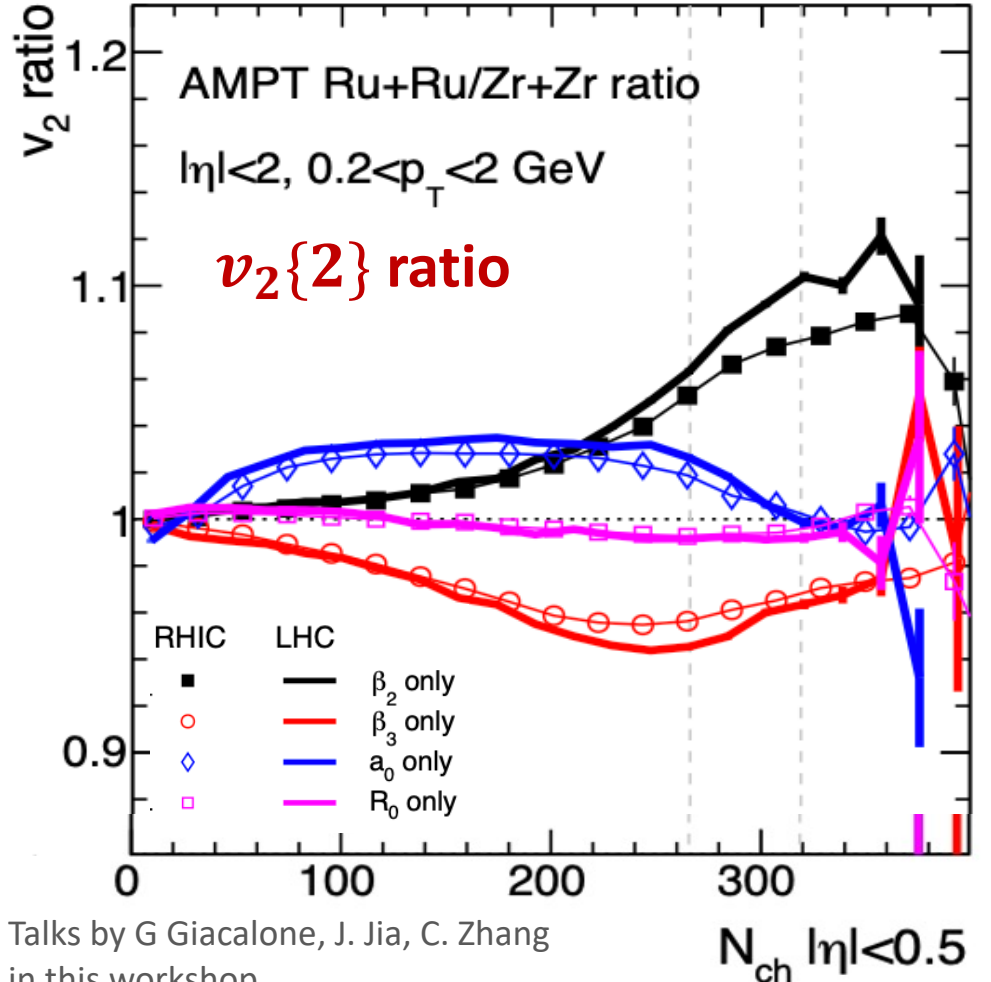
$$v_{2,pp}^2 \propto \epsilon_{2,pp}^2$$



Open Question: **What is the origin of δ_2 ?**
What is the nature of δ_2 ?
What is the impact of δ_2 on isobar v_2 ratios?

1. Probe the variation of δ_2 by varying nuclear structure using isobar collisions as a handle.
2. Check the response of δ_2 to WS parameters at different $\sqrt{s_{NN}}$.

Impact of Woods-saxon parameters on $v_2\{2\}$ ratio



| Cases | β_2 | β_3 | a_0 | R |
|-----------|-----------|-----------|-------|------|
| Ru (def.) | 0.162 | 0 | 0.46 | 5.09 |
| Case 2 | 0.06 | 0 | 0.46 | 5.09 |
| Case 3 | 0.06 | 0.2 | 0.46 | 5.09 |
| Case 4 | 0.06 | 0.2 | 0.52 | 5.09 |
| Zr | 0.06 | 0.2 | 0.52 | 5.02 |

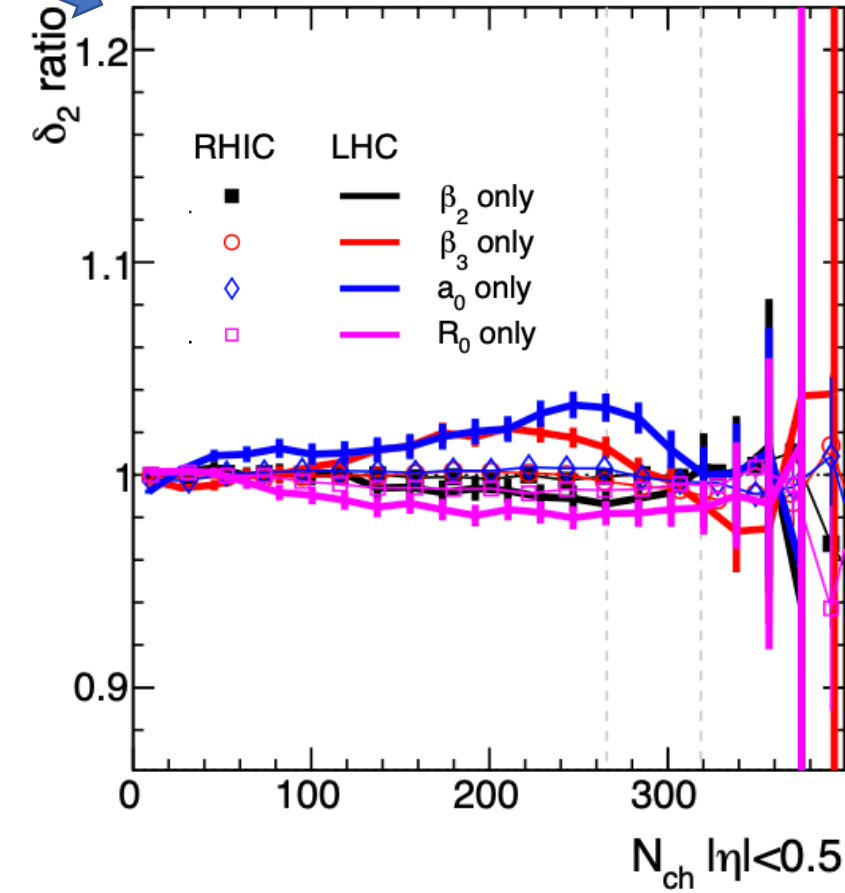
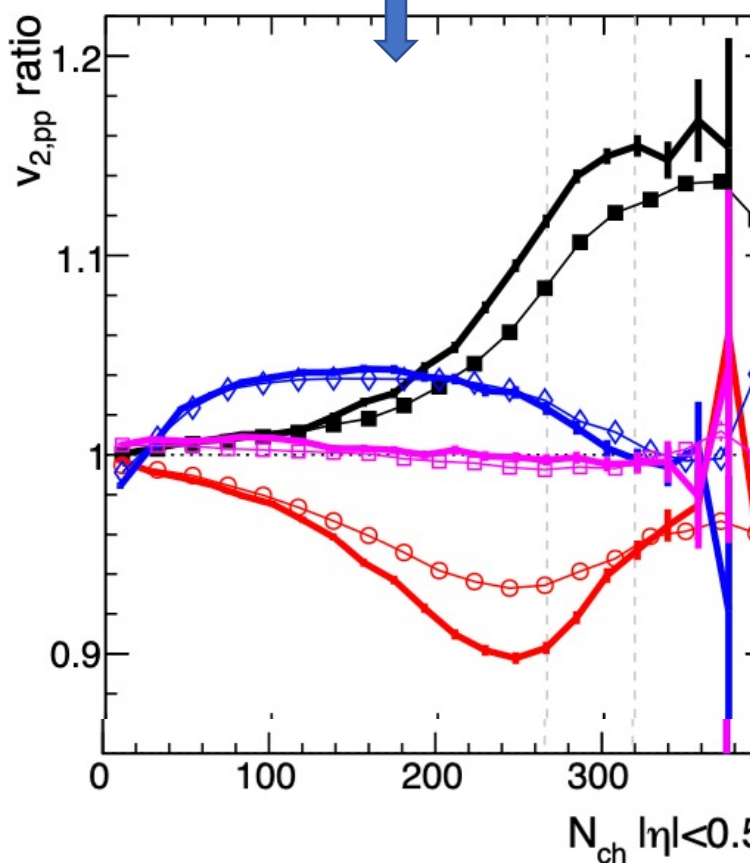
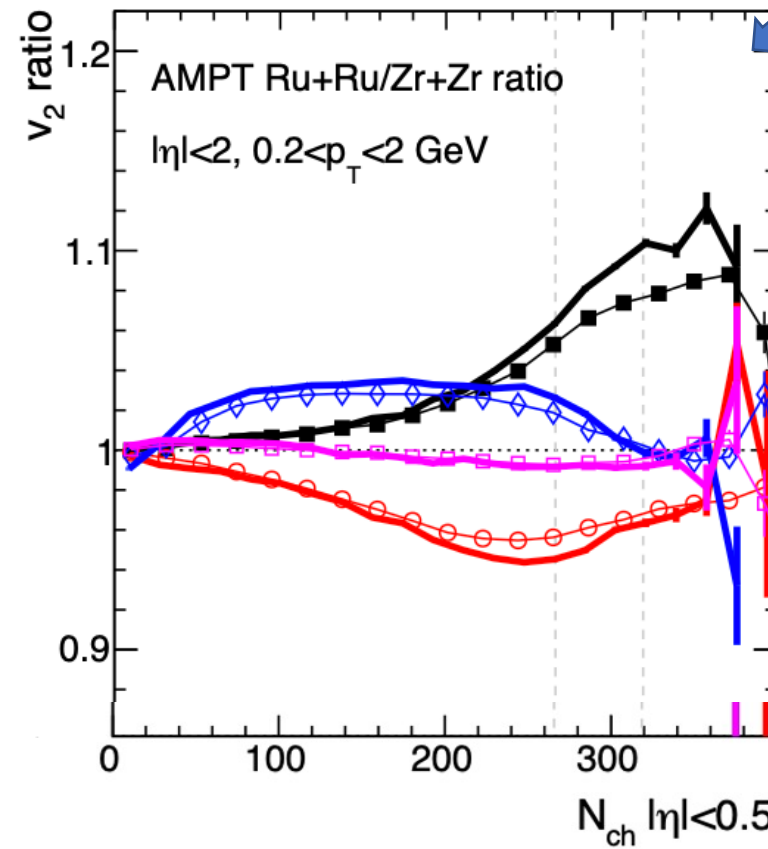
- $\uparrow \beta_2 \Rightarrow \uparrow v_2$, in central events.
- $\uparrow \beta_3 \Rightarrow \uparrow v_2$, in mid-central events.
- $\uparrow a_0 \Rightarrow \downarrow v_2$, in mid-central events.
- $\uparrow R_0$ has small effect(\uparrow) on v_2 in mid-central events.

Talks by G Giacalone, J. Jia, C. Zhang
in this workshop.

- Ratio($v_2\{2\}$) have qualitative agreement between both energies.
- Deformation has a stronger response on Ratio(v_2) at LHC(5 TeV) than at RHIC(200 GeV)

Role of δ_2 on $v_2\{2\}$ Ratio

$$v_2^2\{2\} = v_{2,pp}^2 + \delta_2^2$$



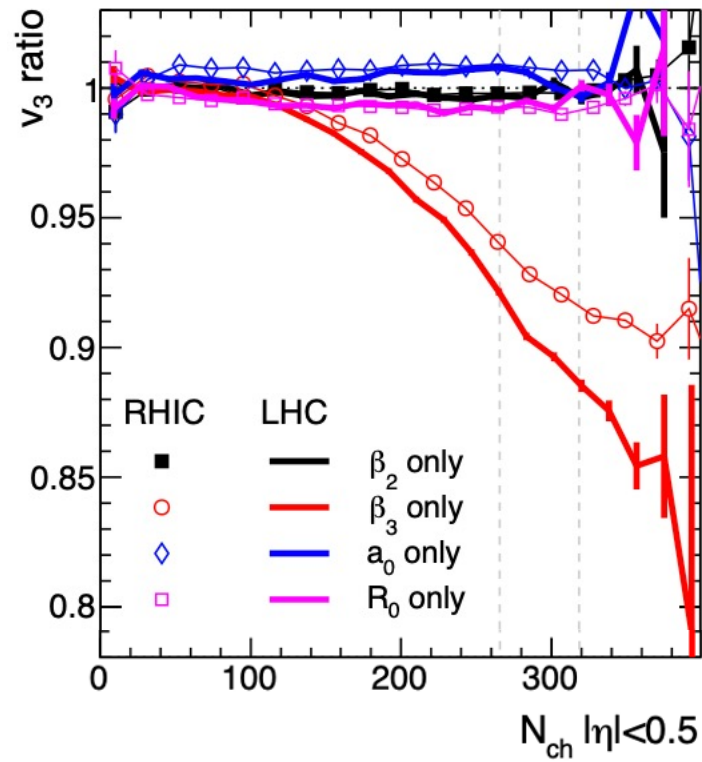
Ratio($v_2\{2\}$) < Ratio($v_{2,pp}$)

Ratio(δ_2) ~ 1 at both energies

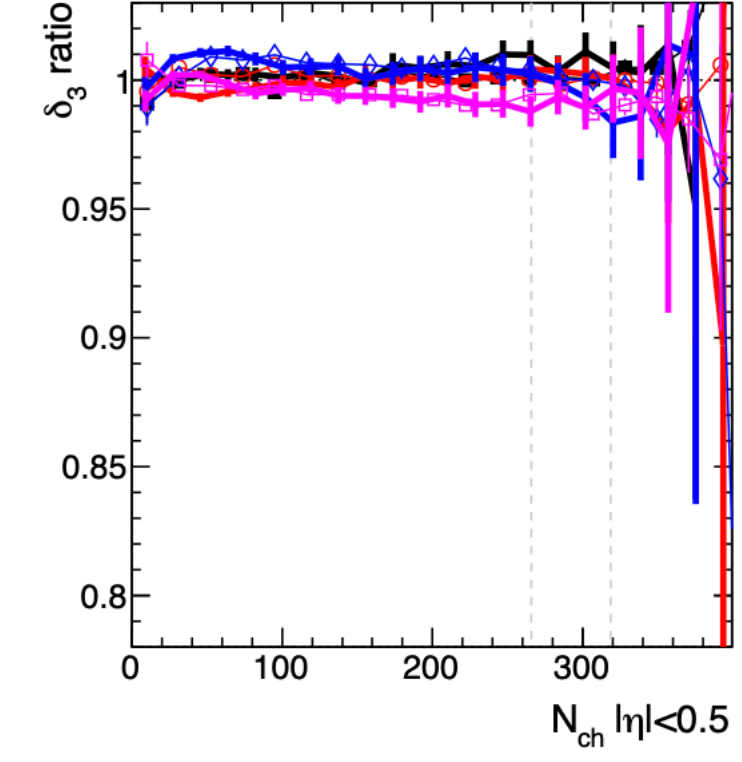
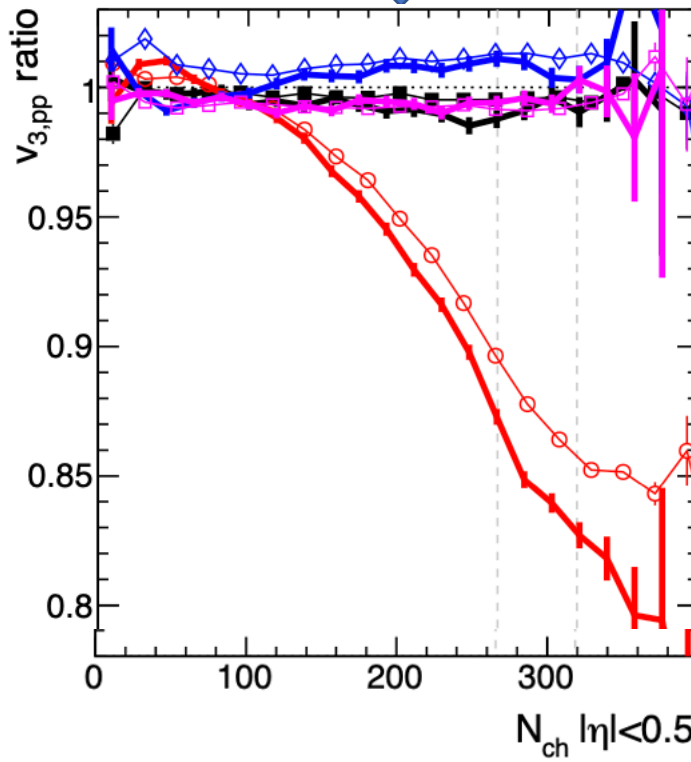
- δ_2 dilutes the impact of initial state participant geometry on final state v_2 .

Role of δ_3 on $v_3\{2\}$ Ratio

$$v_3^2\{2\} = v_{3,pp}^2 + \delta_3^2$$



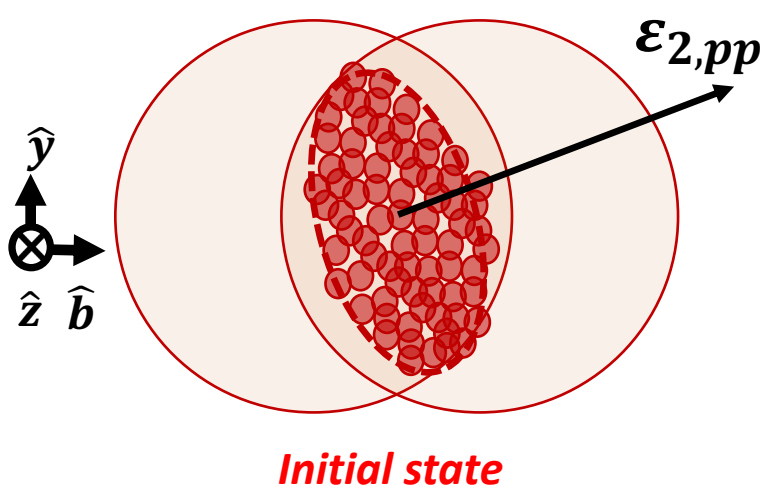
Ratio($v_3\{2\}$) < Ratio($v_{3,pp}$)



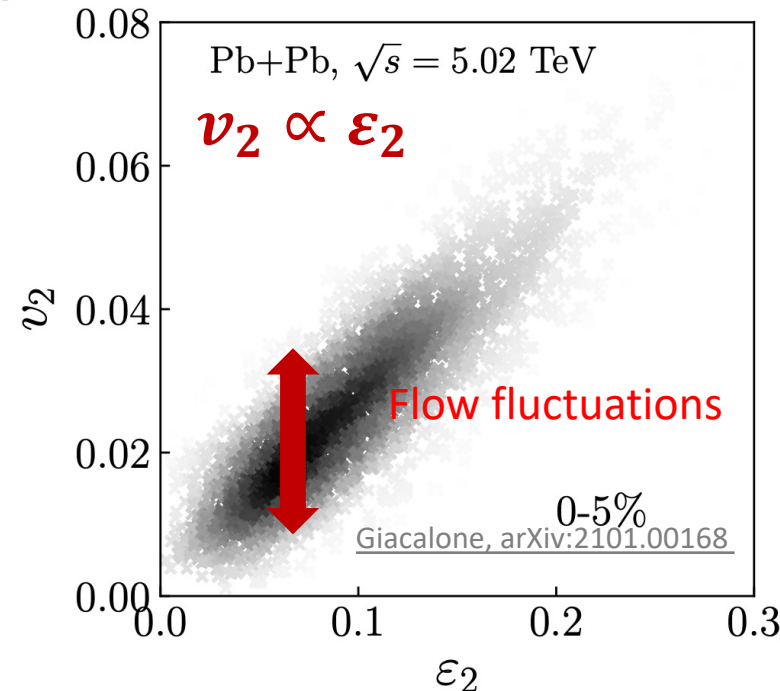
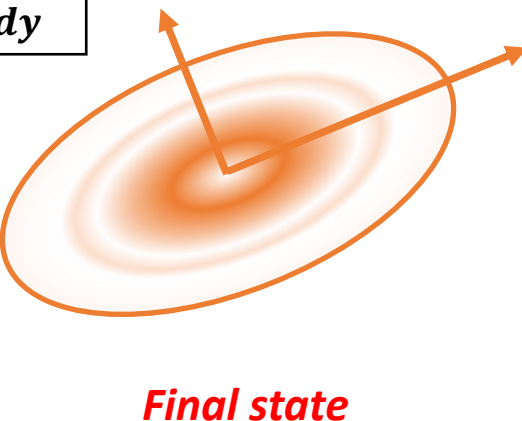
Ratio(δ_3) ~ 1 at both energies

- δ_3 dilutes the impact of initial state participant geometry on final state v_3 .

Conclusion: Role of $\delta_{2,3}$ on $v_{2,3}\{2\}$ Ratio



$$\frac{dP}{dx} > \frac{dP}{dy}$$



$$v_2^2\{2\} = v_{2,pp}^2 + \delta_2^2$$

$\delta_{2,3}$ are not influenced by changing the overall deformation of initial state geometry (even with changing $\sqrt{s_{NN}}$).

- ❖ $\delta_{2,3}$ might originate from:
 1. fluctuations in initial state which are small scale (than global geometry: eg: sub-nucleonic fluc.).
 2. Stochastic effect from final state evolution of system.

- ❖ $\delta_{2,3}$ dilutes the effect of nuclear geometry on final state flow estimates.

PART II:

Response of flow estimates to deformation with varying $\sqrt{s_{NN}}$

Decomposing different contributions to measured $v_2\{2\}$

$$v_2^2\{2\} = \delta_2^2 + v_{2,pp}^2$$

$$v_{2,pp}^2 \propto \varepsilon_{2,pp}^2$$

Decomposing different contributions to measured $v_2\{2\}$

$$v_2^2\{2\} = \delta_2^2 + v_{2,pp}^2$$

$$v_{2,pp}^2 \propto \varepsilon_{2,pp}^2$$

- The initial state eccentricity could have a few independent sources:

$$\varepsilon_{2,pp}^2 = \varepsilon_{2,0}^2 + \varepsilon_{2,rp}^2 + a\beta_2^2 + b\beta_3^2$$

The equation $\varepsilon_{2,pp}^2 = \varepsilon_{2,0}^2 + \varepsilon_{2,rp}^2 + a\beta_2^2 + b\beta_3^2$ is shown above three boxes. A blue arrow points from the first term $\varepsilon_{2,0}^2$ to the box labeled "Fluctuations". Another blue arrow points from the second term $\varepsilon_{2,rp}^2$ to the box labeled "Avg. Geometry". A blue bracket groups the last two terms $a\beta_2^2 + b\beta_3^2$, with a blue arrow pointing from this bracket to the box labeled "Deformations".

Fluctuations

Avg. Geometry

Deformations

Decomposing different contributions to measured $v_2\{2\}$

$$v_2^2\{2\} = \delta_2^2 + v_{2,pp}^2$$

$$v_{2,pp}^2 \propto \varepsilon_{2,pp}^2$$

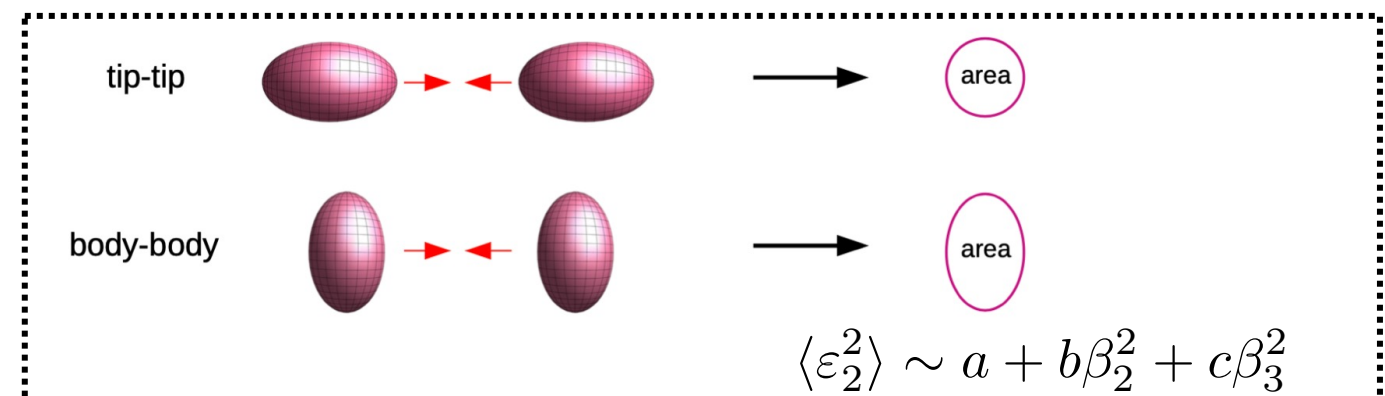
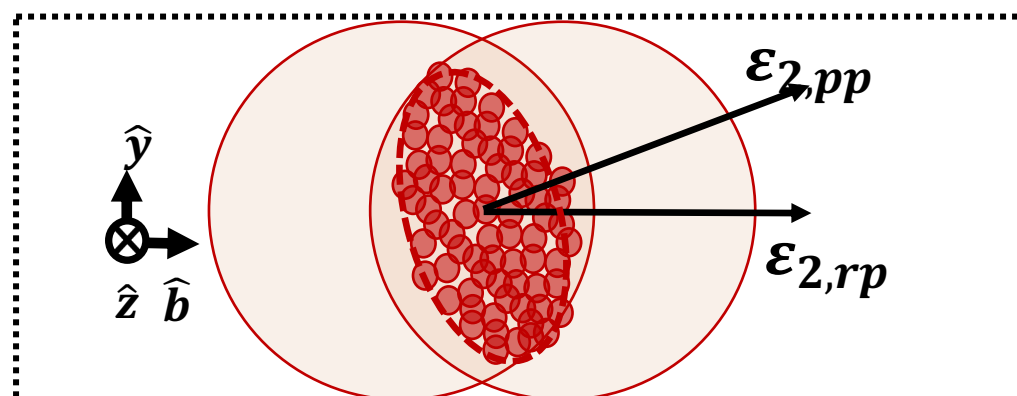
- The initial state eccentricity could have a few independent sources:

$$\varepsilon_{2,pp}^2 = \varepsilon_{2,0}^2 + \varepsilon_{2,rp}^2 + a\beta_2^2 + b\beta_3^2$$

Fluctuations

Avg. Geometry

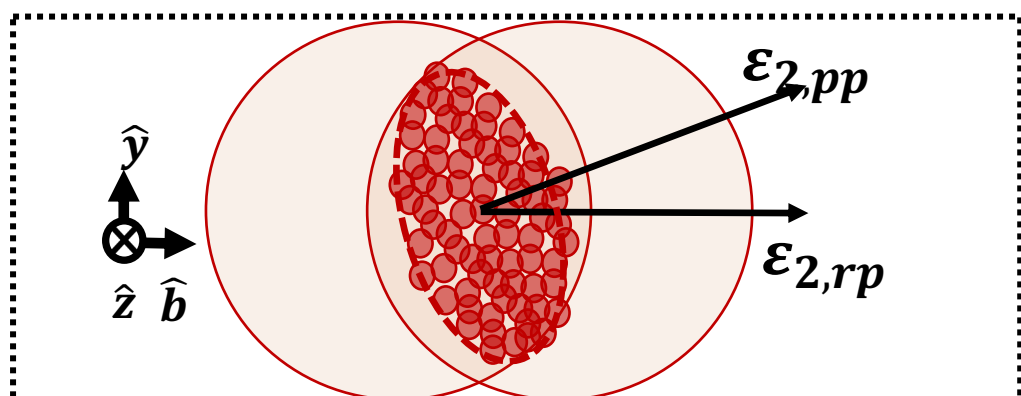
Deformations



Decomposing different contributions to measured $v_2\{2\}$

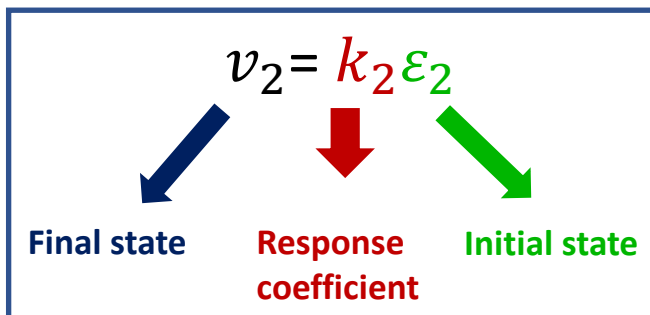
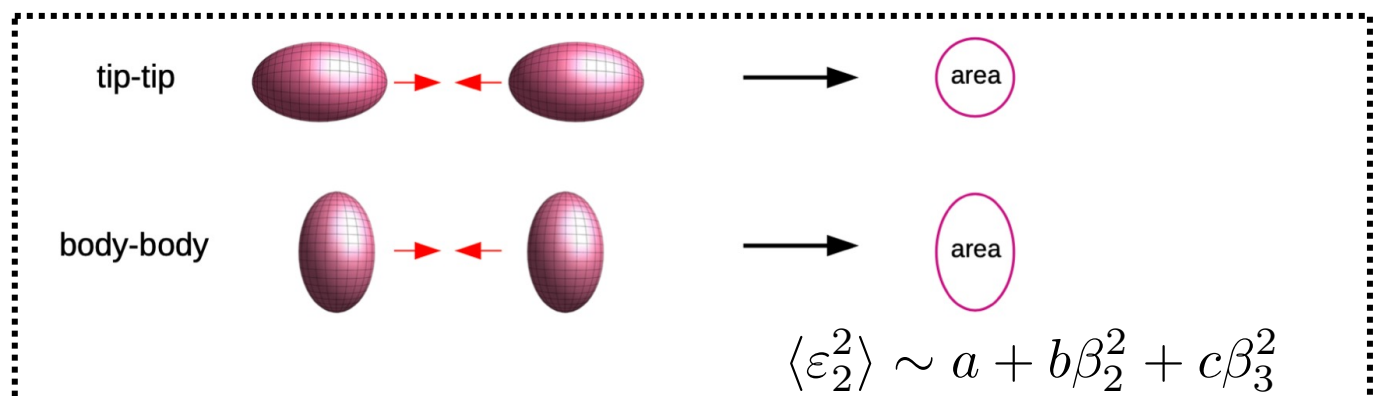
$$v_2^2\{2\} = \delta_2^2 + v_{2,pp}^2$$

- The initial state eccentricity could have a few independent sources:



$$\varepsilon_{2,pp}^2 = \varepsilon_{2,0}^2 + \varepsilon_{2,RP}^2 + a\beta_2^2 + b\beta_3^2$$

Fluctuations Avg. Geometry Deformations



Decomposing different contributions to measured $v_2\{2\}$

$$v_2^2\{2\} = \delta_2^2 + v_{2,pp}^2$$

$$v_{2,pp}^2 \propto \varepsilon_{2,pp}^2$$

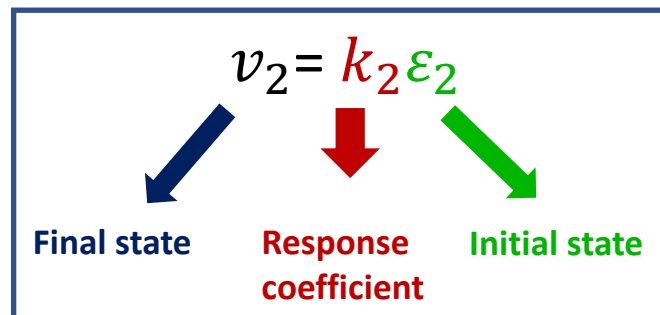
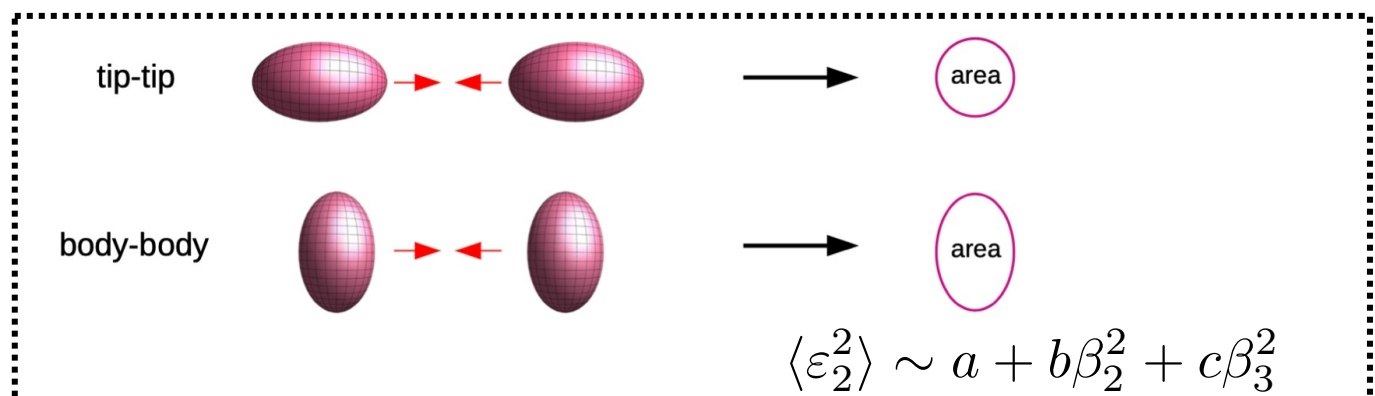
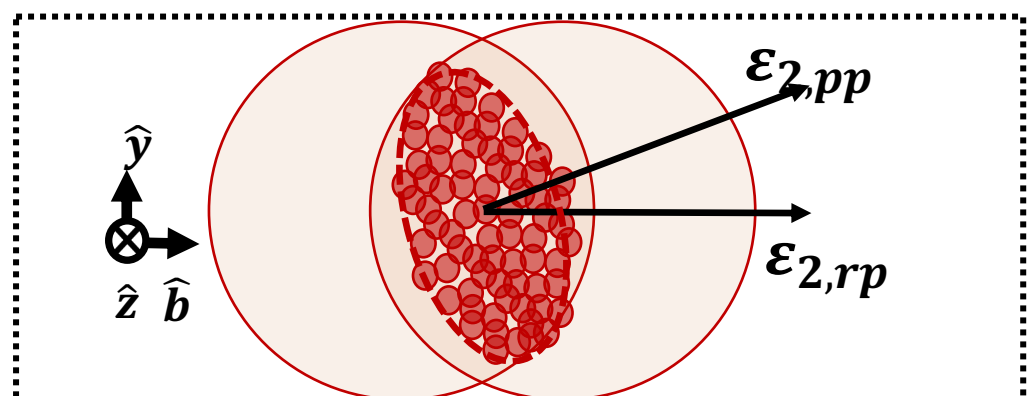
- The initial state eccentricity could have a few independent sources:

$$\varepsilon_{2,pp}^2 = \varepsilon_{2,0}^2 + \varepsilon_{2,rp}^2 + a\beta_2^2 + b\beta_3^2$$

Fluctuations

Avg. Geometry

Deformations



$$v_2^2\{2\} = \delta_2^2 + k_0^2 \varepsilon_{2,0}^2 + k_2\{rp\}^2 \varepsilon_{2,rp}^2 + k_2\{\beta_2\}^2 a\beta_2^2 + k_2\{\beta_3\}^2 b\beta_3^2$$

Decomposing different contributions to measured $v_2\{2\}$

$$v_2^2\{2\} = \delta_2^2 + v_{2,pp}^2$$

$$v_{2,pp}^2 \propto \varepsilon_{2,pp}^2$$

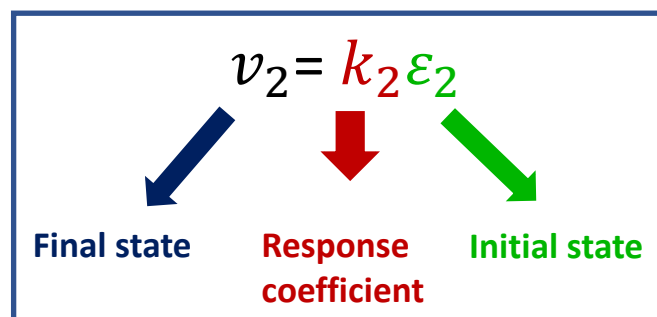
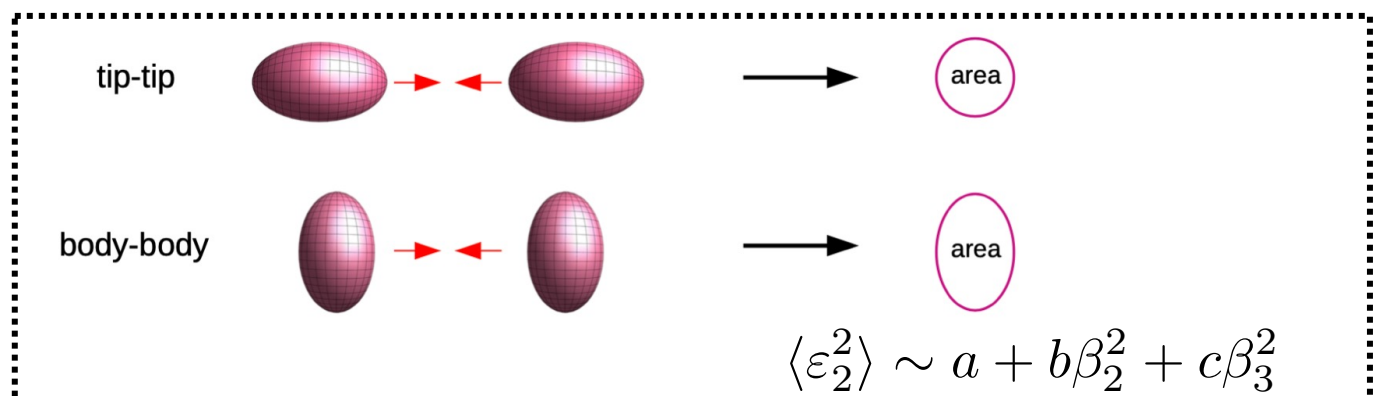
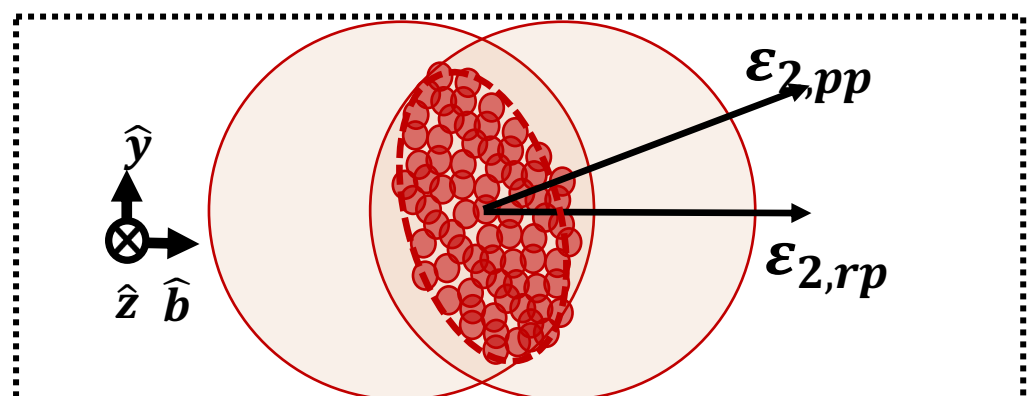
- The initial state eccentricity could have a few independent sources:

$$\varepsilon_{2,pp}^2 = \varepsilon_{2,0}^2 + \varepsilon_{2,rp}^2 + a\beta_2^2 + b\beta_3^2$$

Fluctuations

Avg. Geometry

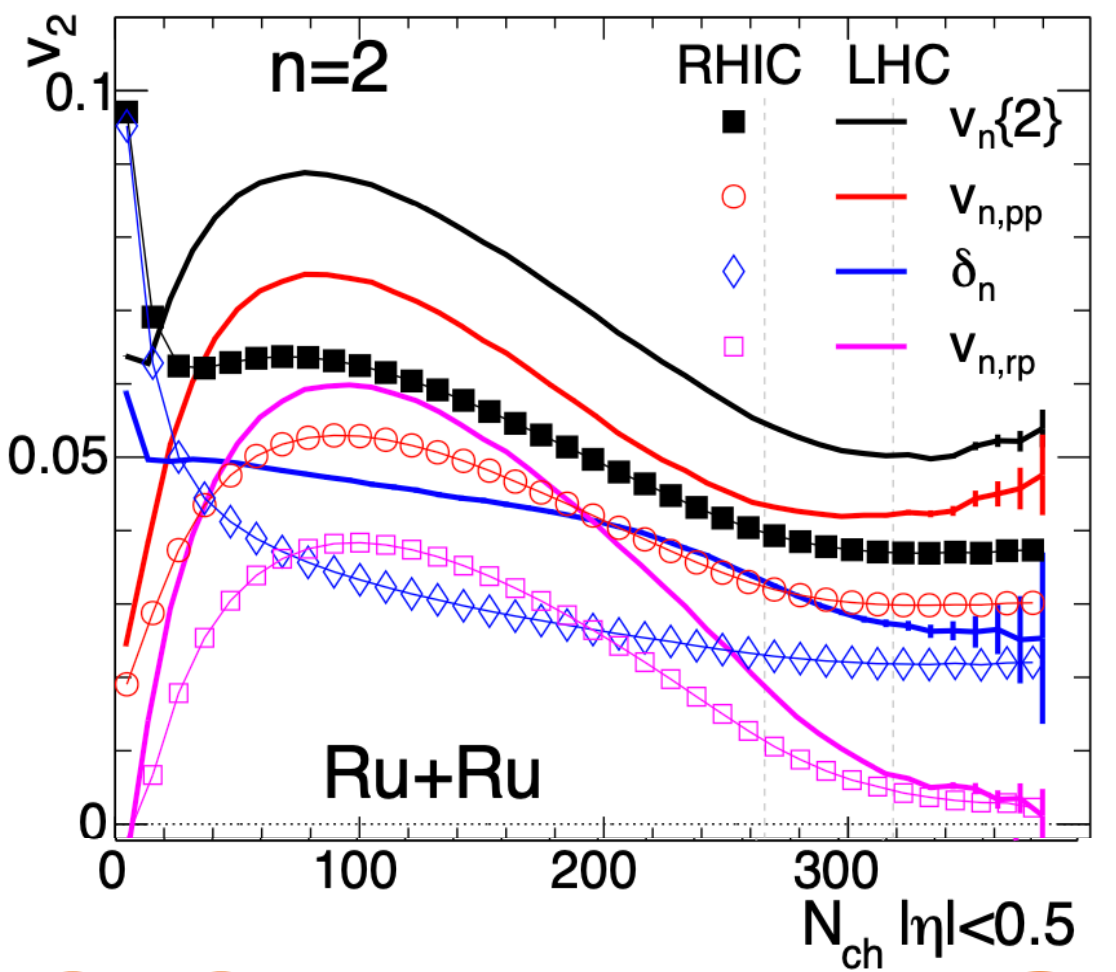
Deformations



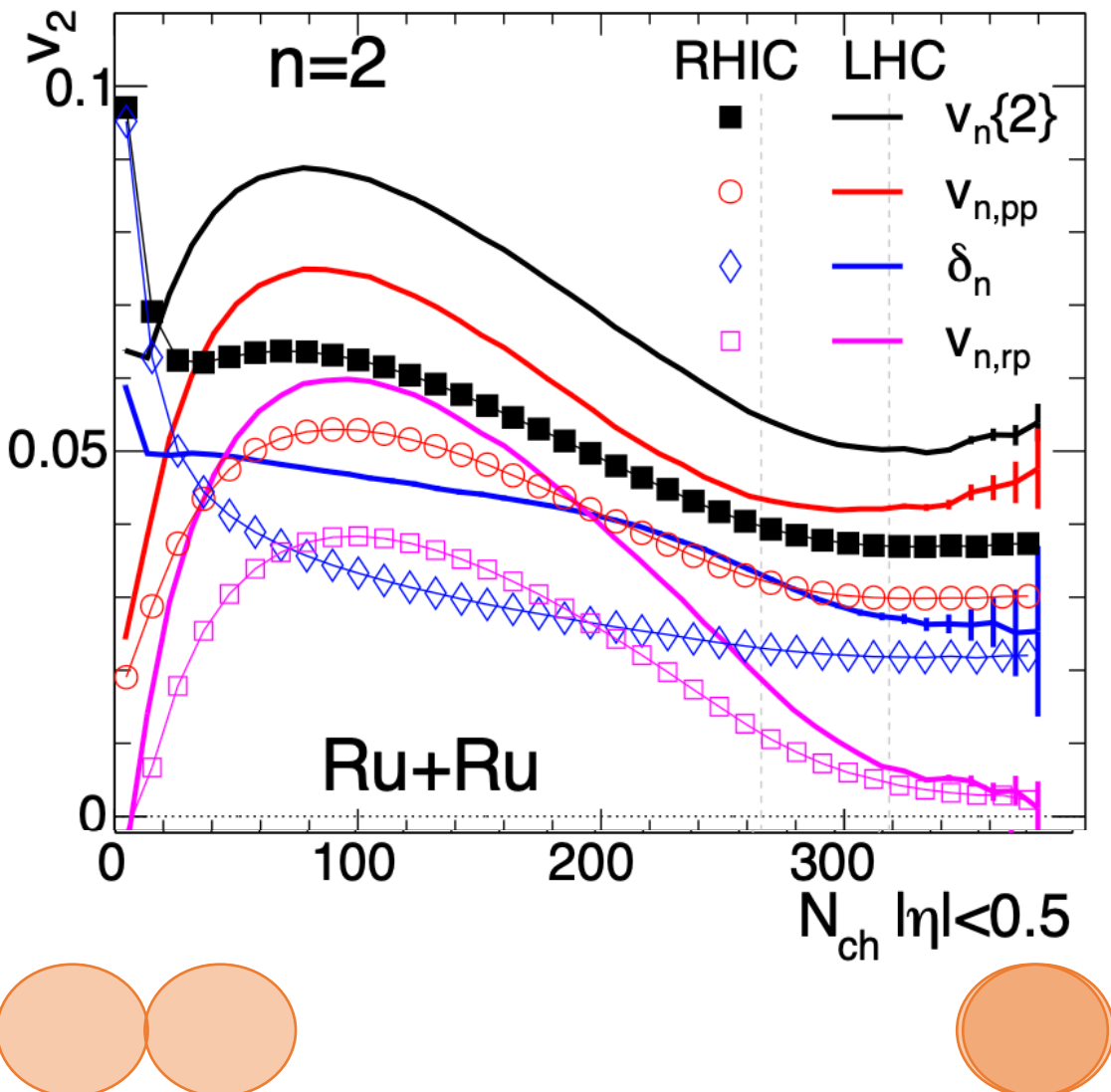
$$v_2^2\{2\} = \delta_2^2 + k_0^2 \varepsilon_{2,0}^2 + k_2\{rp\}^2 \varepsilon_{2,rp}^2 + k_2\{\beta_2\}^2 a\beta_2^2 + k_2\{\beta_3\}^2 b\beta_3^2$$

$v_{2,RP}^2$ $v_2\{\beta_2\}^2$ $v_2\{\beta_3\}^2$

v_2 comparison: 200 GeV and 5 TeV



v_2 comparison: 200 GeV and 5 TeV



- $v_{2,LHC} \geq v_{2,RHIC}$: More frequent partonic scattering.
- Observation: $v_2\{2\} > v_{2,pp} > v_{2,rp}$.

$$v_2^2\{2\} = v_{2,pp}^2 + \delta_2^2$$

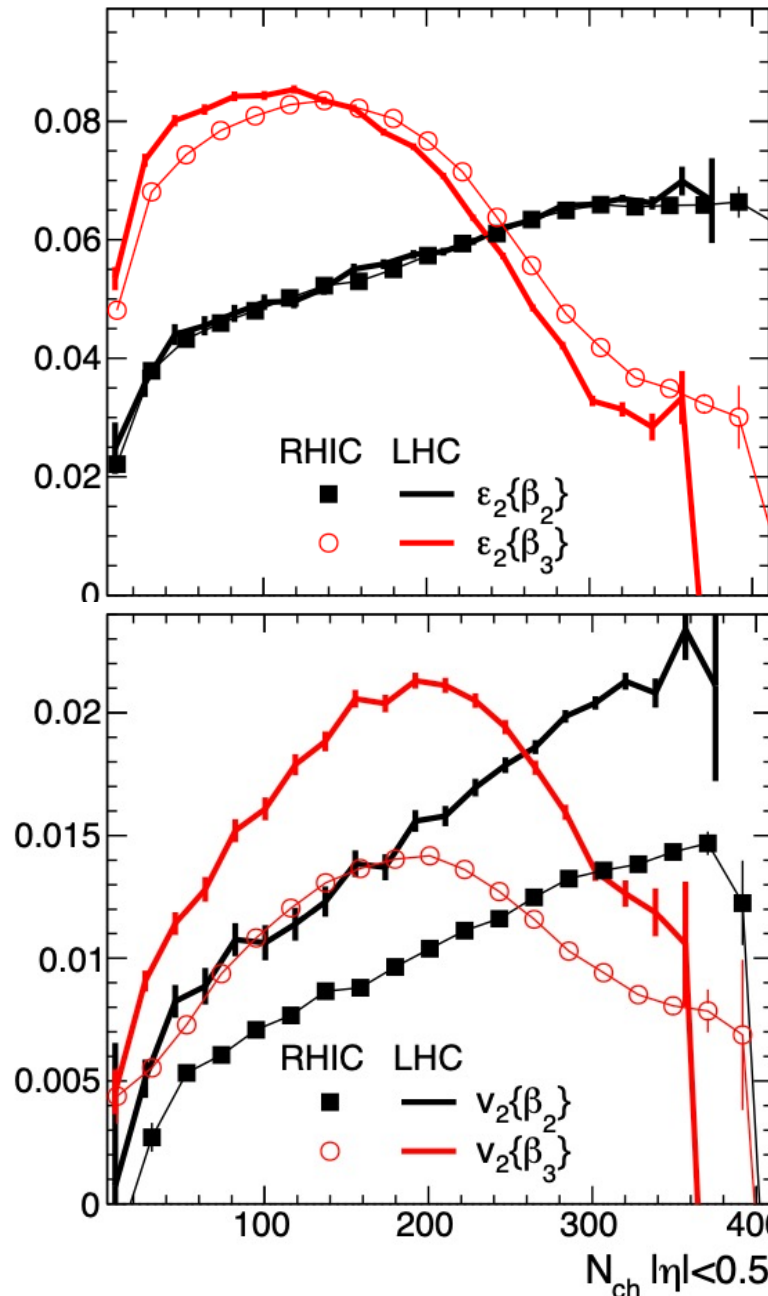
Flow originating from participant geometry.

Part of flow uncorrelated to participant geometry.

❖ δ_2 comparable to $v_{2,pp}$ in central events (!).

“Contribution to final state flow from sources uncorrelated to initial state geometry is as large as those arising from initial state geometry itself!”

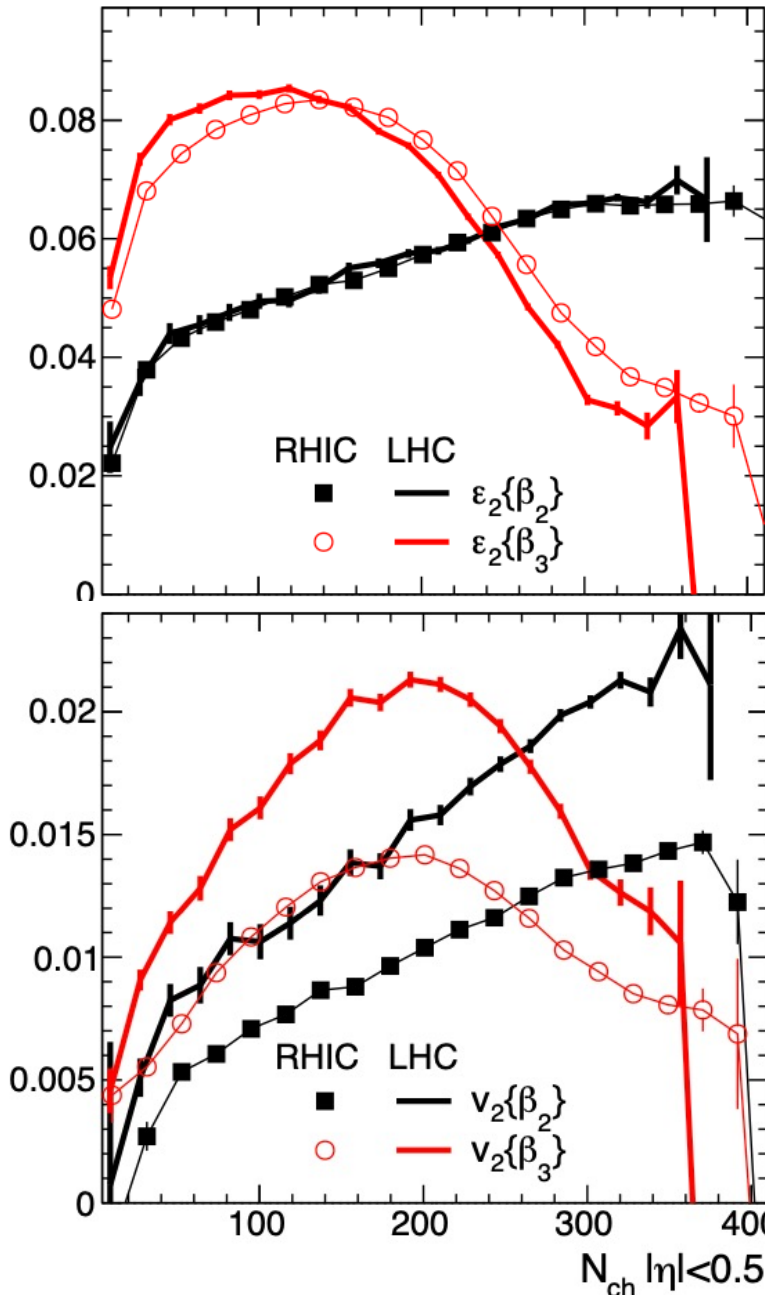
Evolution of Impact of deformation on ε_2 and $v_2\{\beta\}$



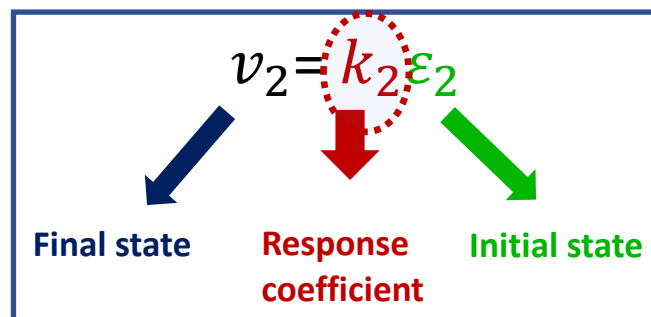
- $\varepsilon_2\{\beta_2\} = \sqrt{a\beta_2^2}$, $\varepsilon_2\{\beta_3\} = \sqrt{b\beta_3^2}$
- Same evolution with N_{ch} at both energies.
- Large differences observed between LHC and RHIC for $v_2\{\beta_2\}$ and $v_2\{\beta_3\}$: Stronger response at LHC.

| Cases | β_2 | β_3 | a_0 | R |
|-----------|-----------|-----------|-------|------|
| Ru (def.) | 0.162 | 0 | 0.46 | 5.09 |
| Case 2 | 0.06 | 0 | 0.46 | 5.09 |
| Case 3 | 0.06 | 0.2 | 0.46 | 5.09 |
| Case 4 | 0.06 | 0.2 | 0.52 | 5.09 |
| Zr | 0.06 | 0.2 | 0.52 | 5.02 |

Evolution of Impact of deformation on ε_2 and $v_2\{\beta\}$

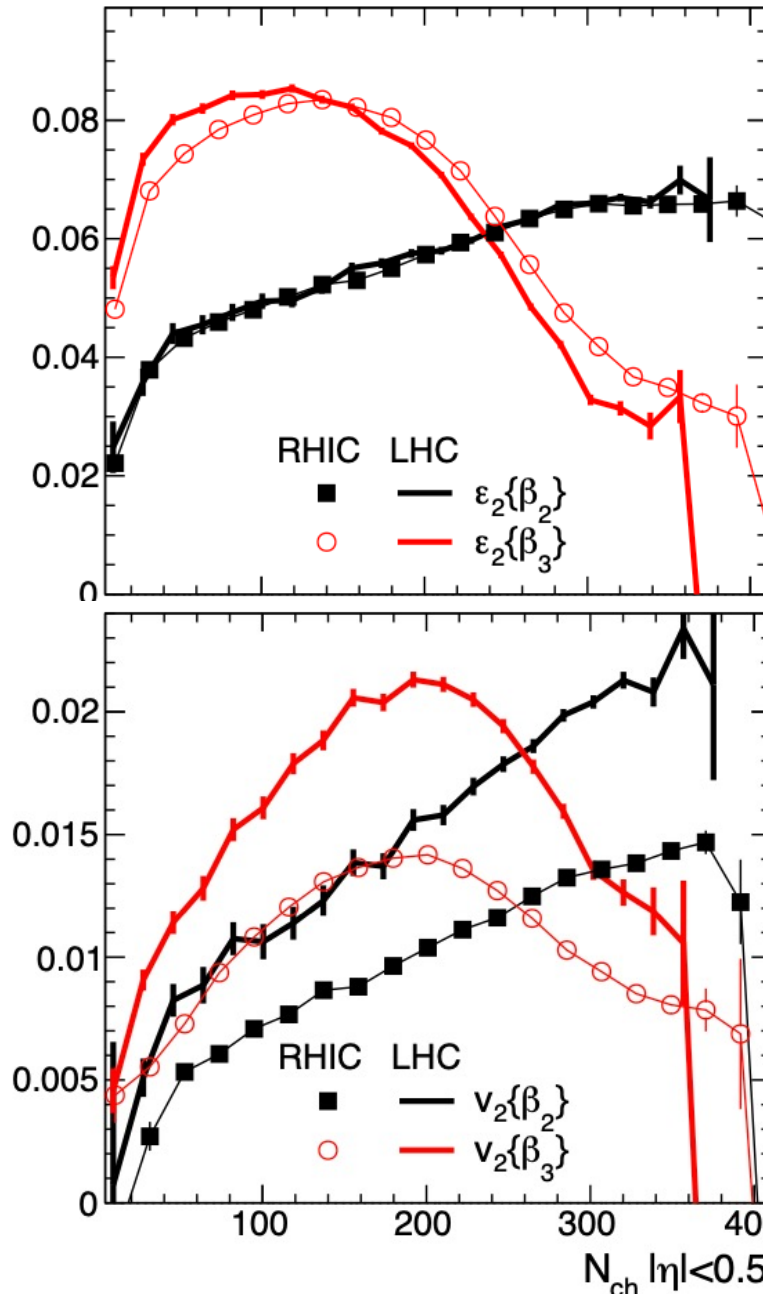


- $\varepsilon_2\{\beta_2\} = \sqrt{a\beta_2^2}$, $\varepsilon_2\{\beta_3\} = \sqrt{b\beta_3^2}$
- Same evolution with Nch at both energies.
- Large differences observed between LHC and RHIC for $v_2\{\beta_2\}$ and $v_2\{\beta_3\}$: Stronger response at LHC.

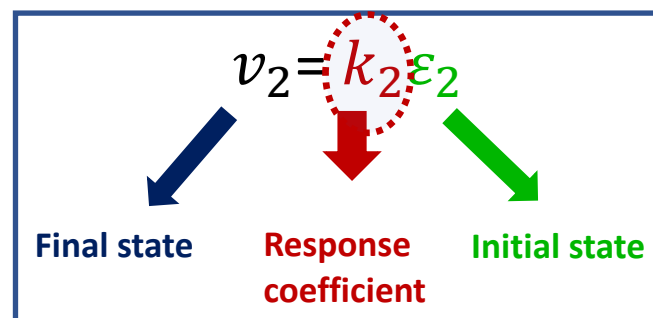


| Cases | β_2 | β_3 | a_0 | R |
|-----------|-----------|-----------|-------|------|
| Ru (def.) | 0.162 | 0 | 0.46 | 5.09 |
| Case 2 | 0.06 | 0 | 0.46 | 5.09 |
| Case 3 | 0.06 | 0.2 | 0.46 | 5.09 |
| Case 4 | 0.06 | 0.2 | 0.52 | 5.09 |
| Zr | 0.06 | 0.2 | 0.52 | 5.02 |

Evolution of Impact of deformation on ε_2 and $v_2\{\beta\}$



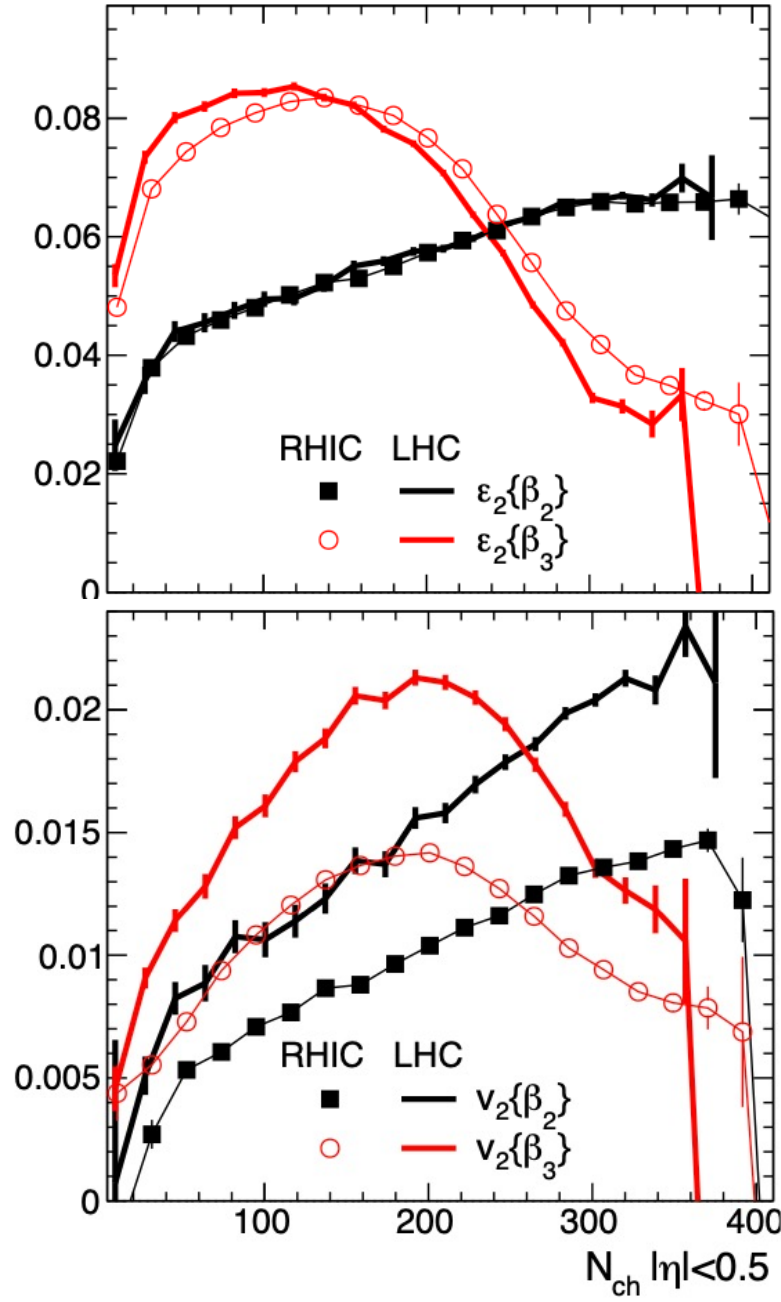
- $\varepsilon_2\{\beta_2\} = \sqrt{a\beta_2^2}$, $\varepsilon_2\{\beta_3\} = \sqrt{b\beta_3^2}$
- Same evolution with Nch at both energies.
- Large differences observed between LHC and RHIC for $v_2\{\beta_2\}$ and $v_2\{\beta_3\}$: Stronger response at LHC.



➤ How does k_2 for different components of flow evolve with $\sqrt{s_{NN}}$?

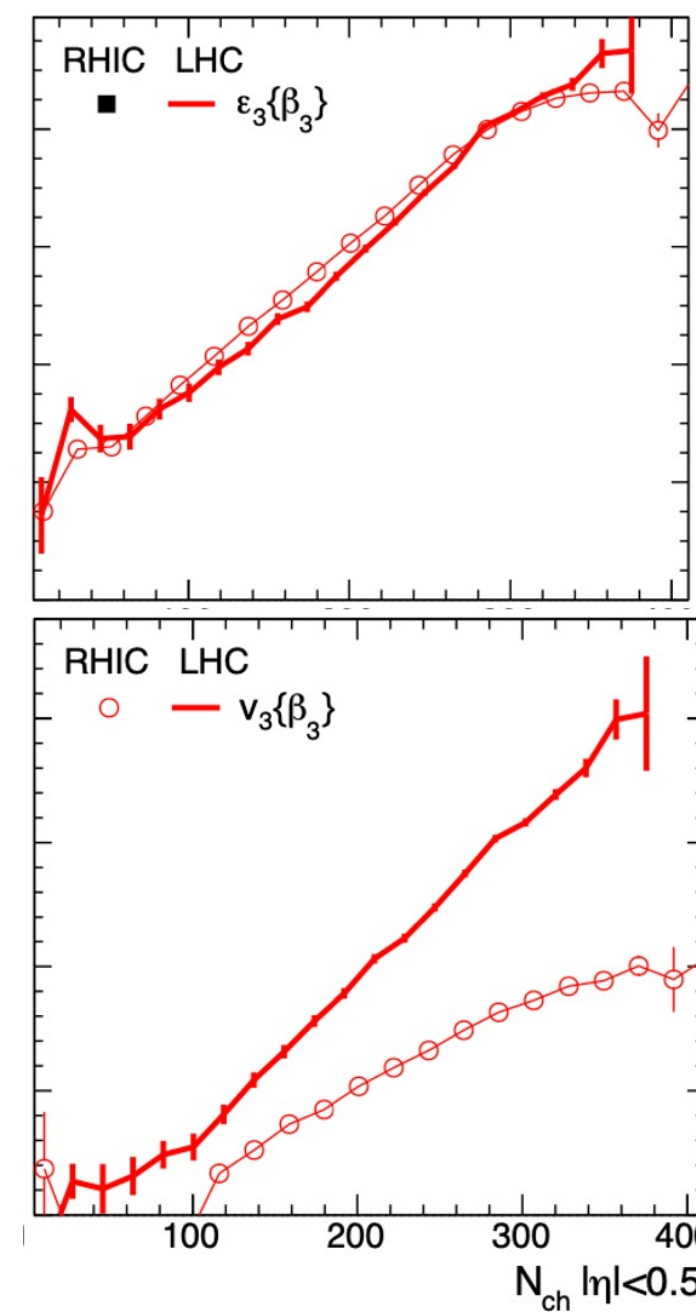
| Cases | β_2 | β_3 | a_0 | R |
|-----------|-----------|-----------|-------|------|
| Ru (def.) | 0.162 | 0 | 0.46 | 5.09 |
| Case 2 | 0.06 | 0 | 0.46 | 5.09 |
| Case 3 | 0.06 | 0.2 | 0.46 | 5.09 |
| Case 4 | 0.06 | 0.2 | 0.52 | 5.09 |
| Zr | 0.06 | 0.2 | 0.52 | 5.02 |

Evolution of Impact of deformation on ε_2 and $v_2\{\cdot\}$



$$k_2\{\beta_2\} = \frac{v_2\{\beta_2\}}{\varepsilon_2\{\beta_2\}}$$

$$k_2\{\beta_3\} = \frac{v_2\{\beta_3\}}{\varepsilon_2\{\beta_3\}}$$



$$k_3\{\beta_3\} = \frac{v_3\{\beta_3\}}{\varepsilon_3\{\beta_3\}}$$

$\sqrt{s_{NN}}$ evolution of response coefficients

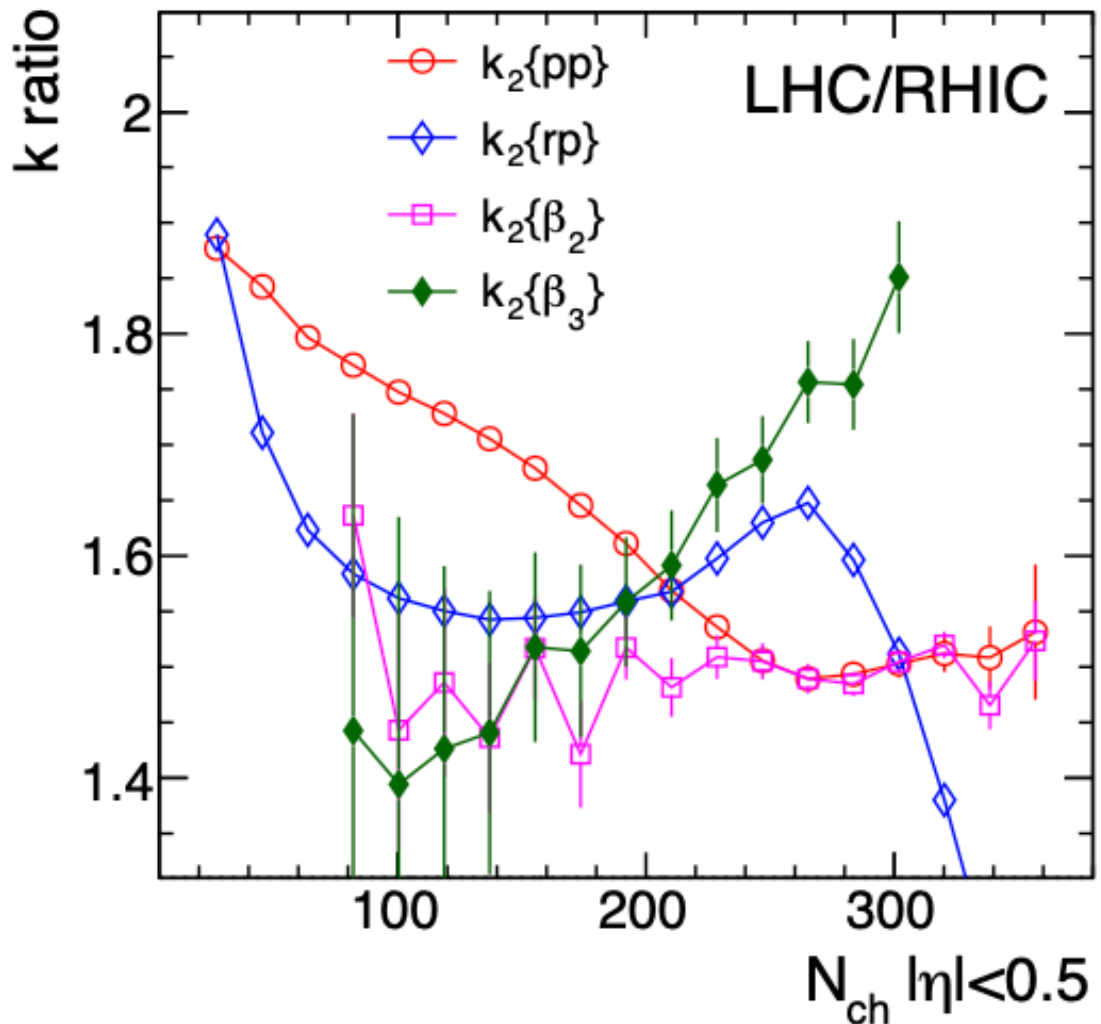
$$v_2^2\{2\} = \delta_2^2 + k_0^2 \varepsilon_{2,0}^2 + k_2\{rp\}^2 \varepsilon_{2,rp}^2 + k_2\{\beta_2\}^2 a \beta_2^2 + k_2\{\beta_3\}^2 b \beta_3^2$$

$$k_2\{pp\} = \frac{v_{2,pp}}{\varepsilon_{2,pp}} \quad k_2\{rp\} = \frac{v_{2,rp}}{\varepsilon_{2,rp}}$$

$$k_2\{\beta_2\} = \frac{v_2\{\beta_2\}}{\varepsilon_2\{\beta_2\}} \quad k_2\{\beta_3\} = \frac{v_2\{\beta_3\}}{\varepsilon_2\{\beta_3\}}$$

$\sqrt{s_{NN}}$ evolution of response coefficients

$$v_2^2\{2\} = \delta_2^2 + k_0^2 \varepsilon_{2,0}^2 + k_2\{rp\}^2 \varepsilon_{2,rp}^2 + k_2\{\beta_2\}^2 a \beta_2^2 + k_2\{\beta_3\}^2 b \beta_3^2$$

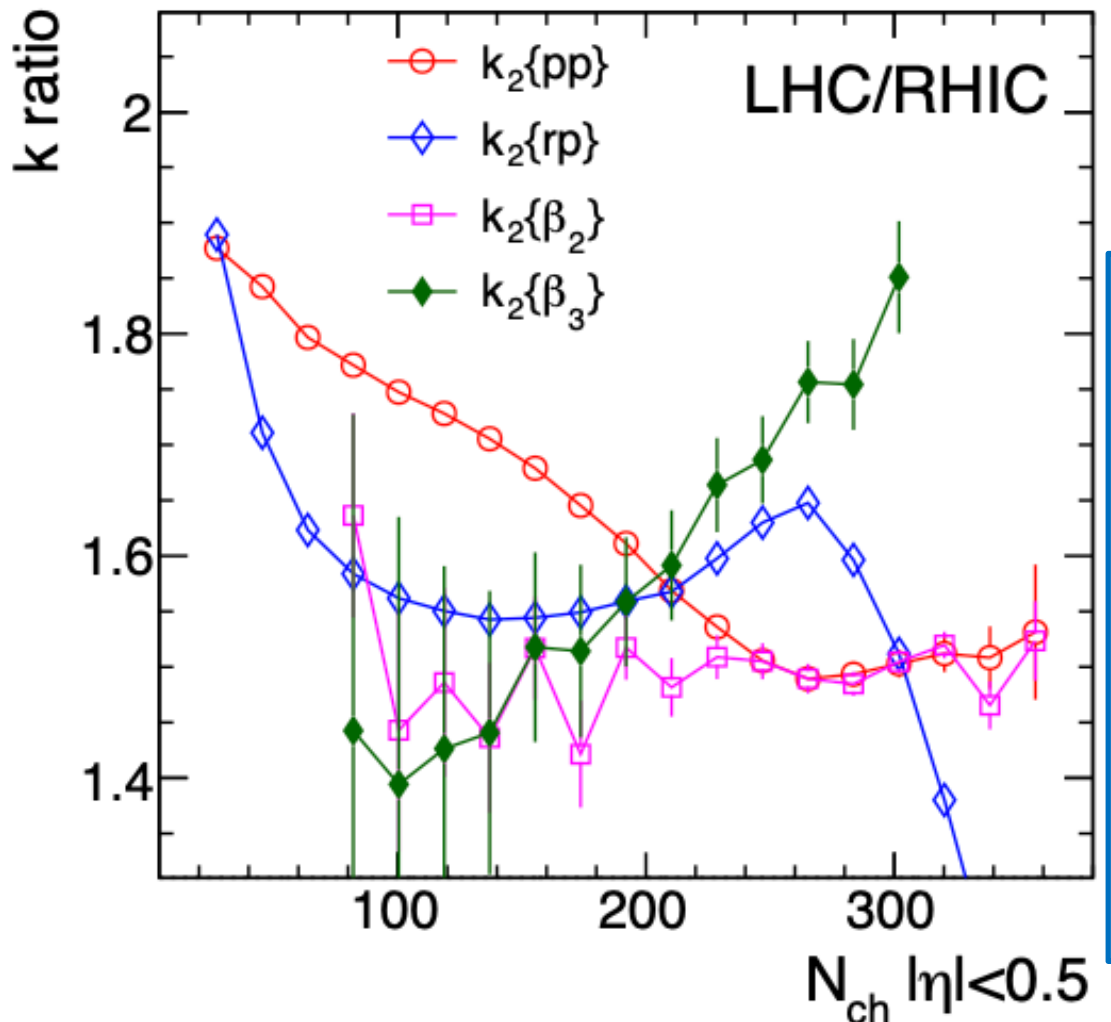


$$k_2\{pp\} = \frac{v_{2,pp}}{\varepsilon_{2,pp}} \quad k_2\{rp\} = \frac{v_{2,rp}}{\varepsilon_{2,rp}}$$

$$k_2\{\beta_2\} = \frac{v_2\{\beta_2\}}{\varepsilon_2\{\beta_2\}} \quad k_2\{\beta_3\} = \frac{v_2\{\beta_3\}}{\varepsilon_2\{\beta_3\}}$$

$\sqrt{s_{NN}}$ evolution of response coefficients

$$v_2^2\{2\} = \delta_2^2 + k_0^2 \varepsilon_{2,0}^2 + k_2\{rp\}^2 \varepsilon_{2,rp}^2 + k_2\{\beta_2\}^2 a \beta_2^2 + k_2\{\beta_3\}^2 b \beta_3^2$$



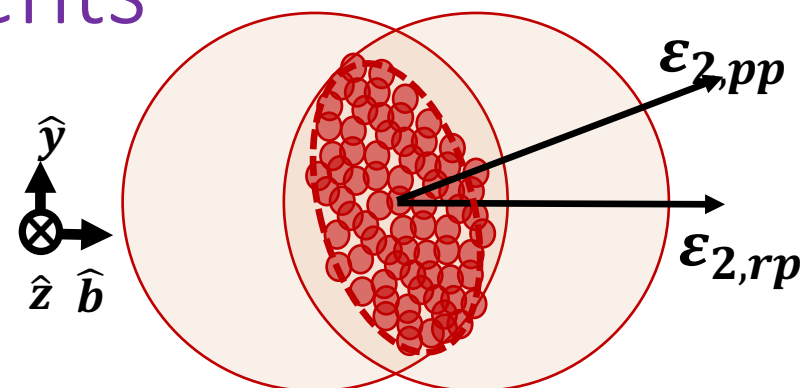
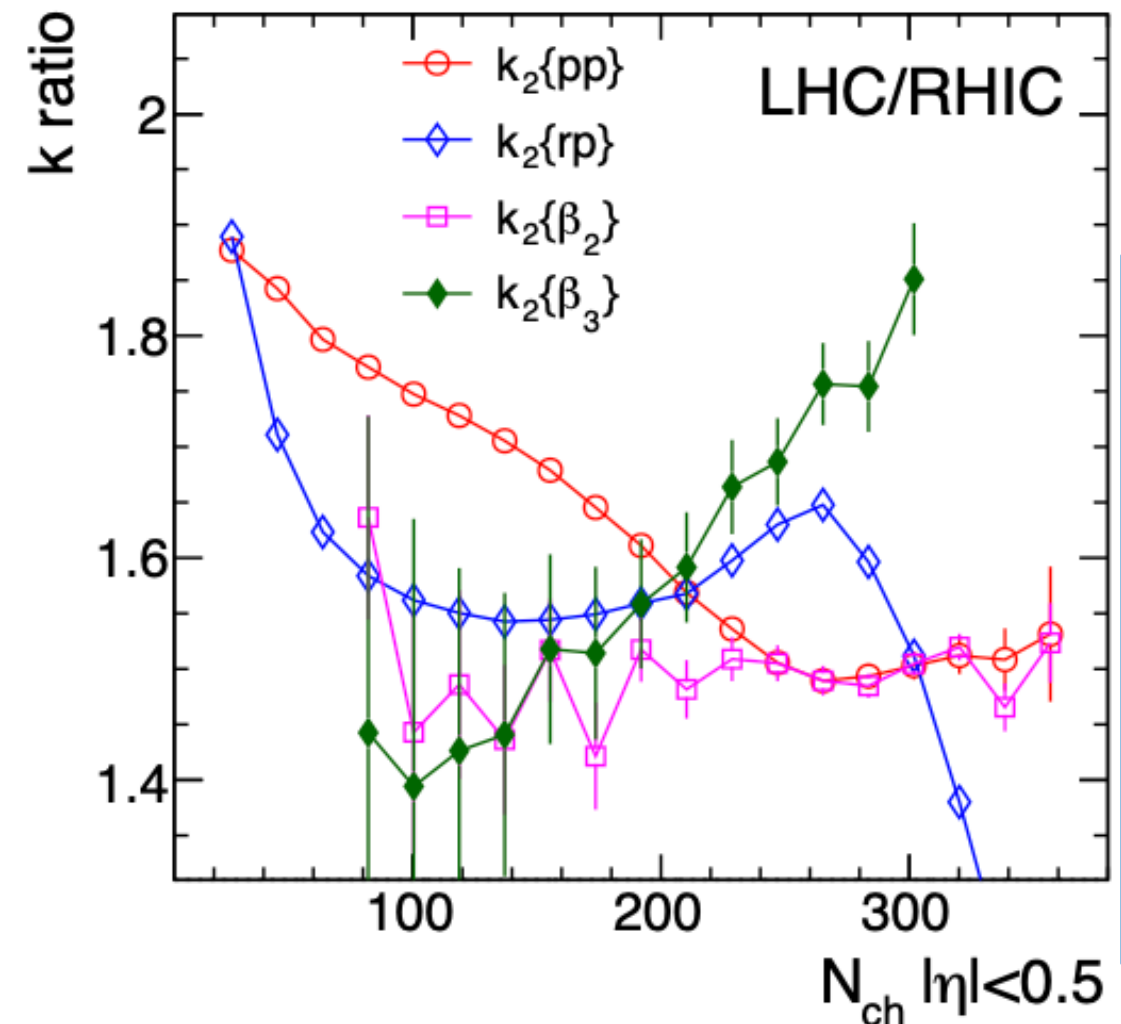
$$k_2\{pp\} = \frac{v_{2,pp}}{\varepsilon_{2,pp}} \quad k_2\{rp\} = \frac{v_{2,rp}}{\varepsilon_{2,rp}}$$

$$k_2\{\beta_2\} = \frac{v_2\{\beta_2\}}{\varepsilon_2\{\beta_2\}} \quad k_2\{\beta_3\} = \frac{v_2\{\beta_3\}}{\varepsilon_2\{\beta_3\}}$$

Observations

1. All k_2 Ratio(LHC/RHIC) > 1: $v_{2,LHC} > v_{2,RHIC}$.
2. Ratio($k_2\{rp\}$) minimum in central events.
3. Ratio($k_2\{pp\}$) largest in mid-central.
4. Ratio($k_2\{pp\}$) = Ratio($k_2\{\beta_2\}$) in central events (!).

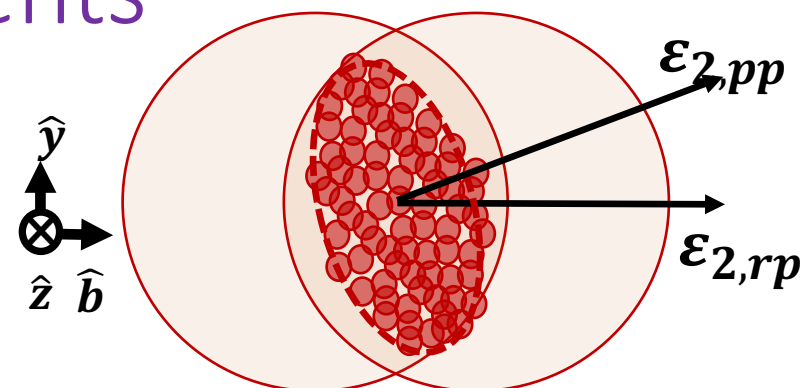
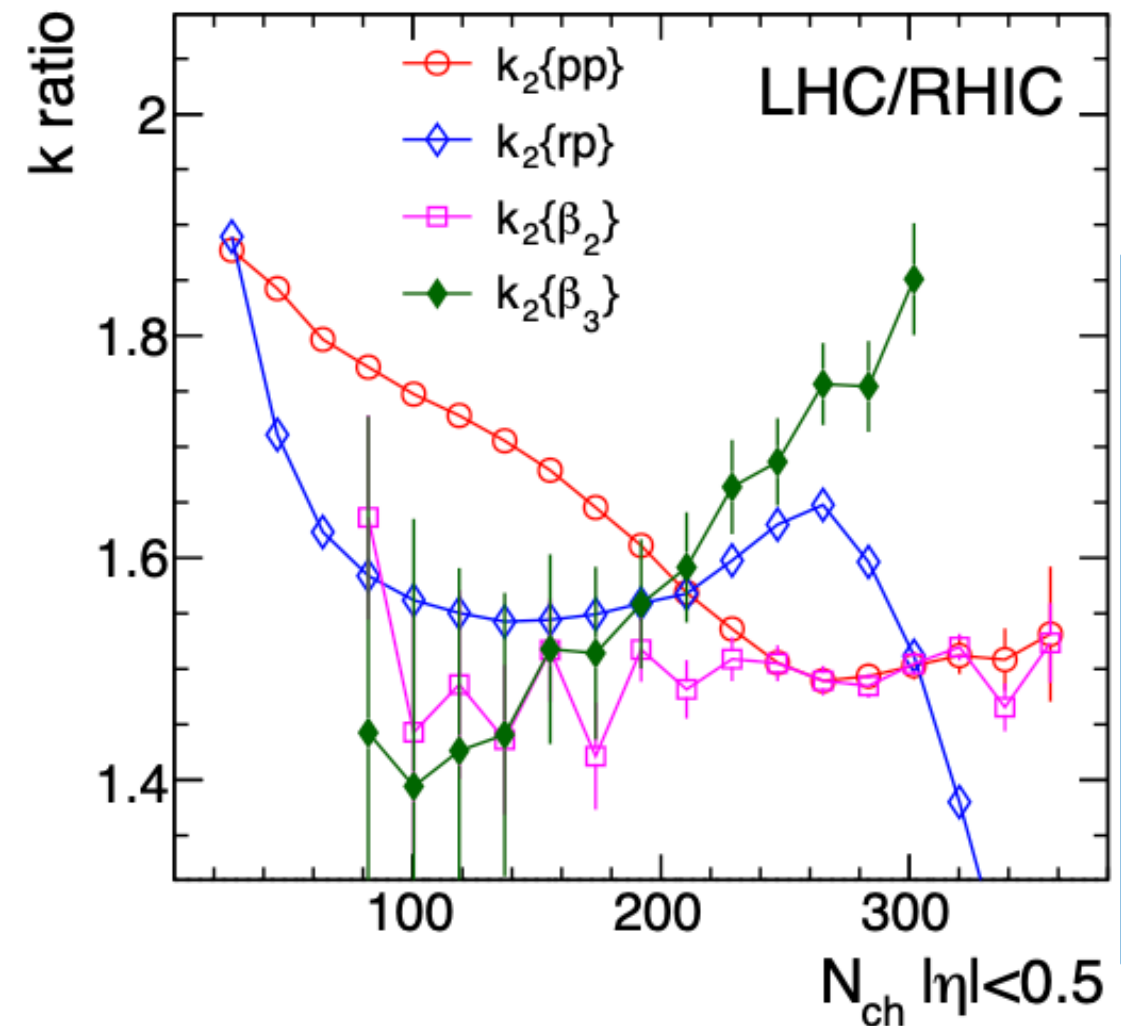
$\sqrt{s_{NN}}$ evolution of response coefficients



Observations

1. All k_2 Ratio(LHC/RHIC) > 1: $v_{2,LHC} > v_{2,RHIC}$.
2. Ratio($k_2\{rp\}$) minimum in central events.
3. Ratio($k_2\{pp\}$) largest in mid-central.
4. Ratio($k_2\{pp\}$) = Ratio($k_2\{\beta_2\}$) in central events (!).

$\sqrt{s_{NN}}$ evolution of response coefficients



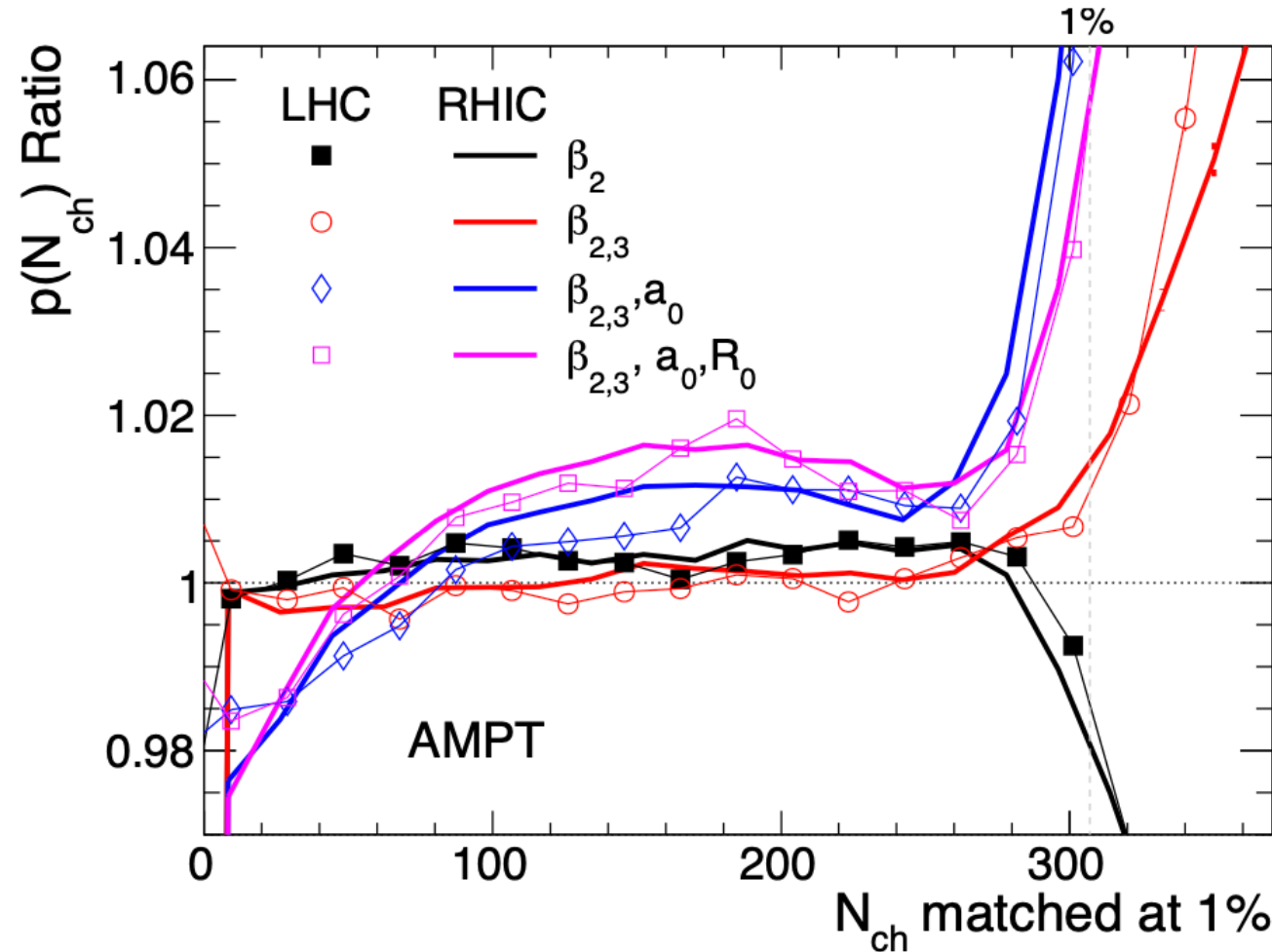
Observations

1. All k_2 Ratio(LHC/RHIC) > 1: $v_{2,LHC} > v_{2,RHIC}$.
2. Ratio($k_2\{rp\}$) minimum in central events.
3. Ratio($k_2\{pp\}$) largest in mid-central.
4. Ratio($k_2\{pp\}$) = Ratio($k_2\{\beta_2\}$) in central events (!).

➤ Difference in Evolution of response coefficients between LHC and RHIC:

Major source of difference in observed flow coefficients in response to same geometry

$p(N_{ch})$ ratio comparison: 200 GeV and 5 TeV



| Cases | β_2 | β_3 | a_0 | R_{38} |
|-----------|-----------|-----------|-------|----------|
| Ru (def.) | 0.162 | 0 | 0.46 | 5.09 |
| Case 2 | 0.06 | 0 | 0.46 | 5.09 |
| Case 3 | 0.06 | 0.2 | 0.46 | 5.09 |
| Case 4 | 0.06 | 0.2 | 0.52 | 5.09 |
| Zr | 0.06 | 0.2 | 0.52 | 5.02 |

- Effect of WS parameters on $p(N_{ch})$ ratios consistent between 200 GeV and 5 TeV.
- The deformation in nuclear geometry impacts $p(N_{ch})$ the same way between the energy scales.

$p(N_{ch})$: robust observable to study effect of nuclear deformation, irrespective of $\sqrt{s_{NN}}$

Conclusion

❖ Using AMPT model, we tried to answer:

Does nuclear deformation manifest same way across energy scales?

❖ We observe:

- At both $\sqrt{s_{NN}}$, $\delta_{2,3}$ dilutes the effect of nuclear geometry on final state flow estimates.
- Even for same nuclear structure; $k_2 \text{ Ratio(LHC/RHIC)} > 1$: results in $v_{2,LHC} > v_{2,RHIC}$.
- $\text{Ratio}(k_2\{pp\}) = \text{Ratio}(k_2\{\beta_2\})$ in central events.
- $p(N_{ch})$ robust observable to study effect of deformation, irrespective of $\sqrt{s_{NN}}$
- ❖ Future Scope: Need further models with saturation physics to disentangle saturation effects and deformation towards eccentricities in initial state and flow in final state.

Backup

Backup

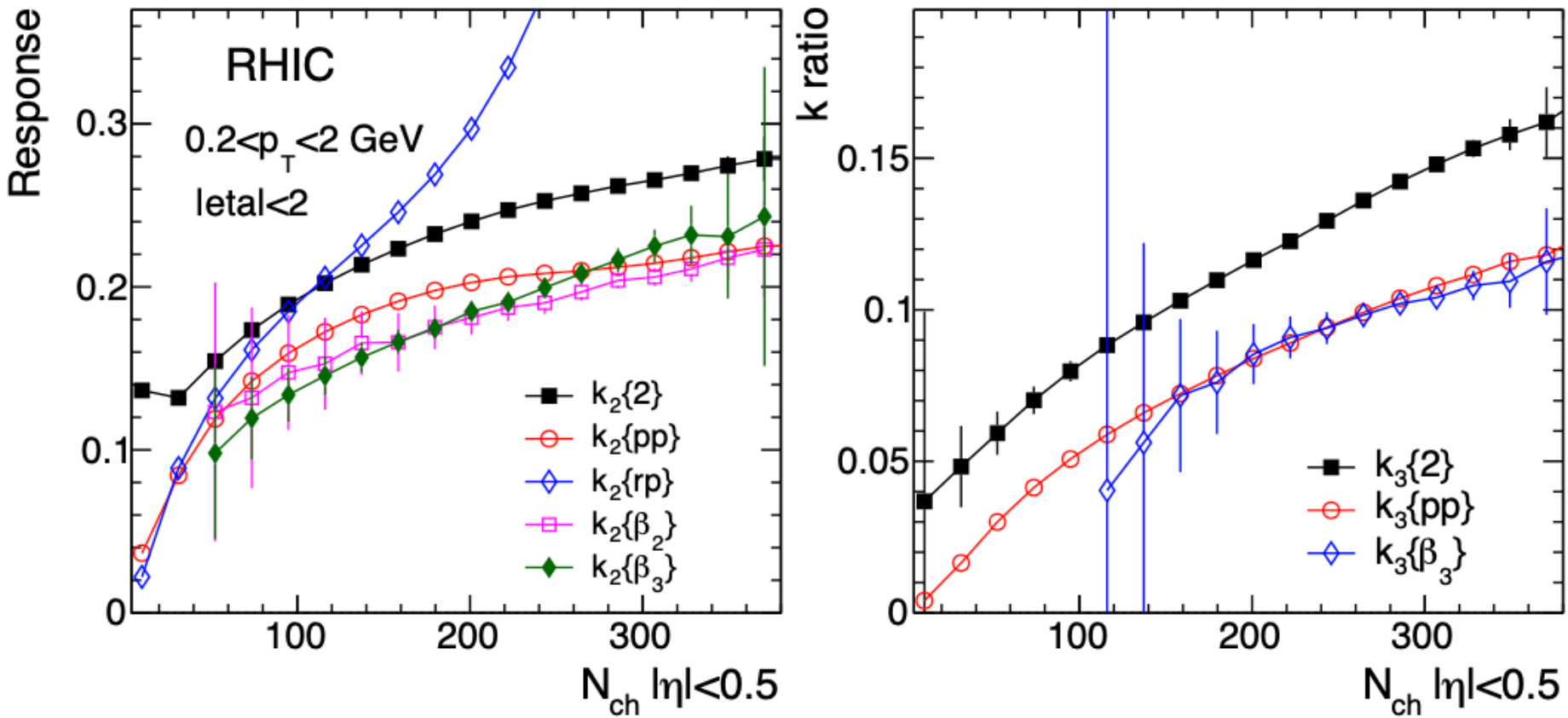
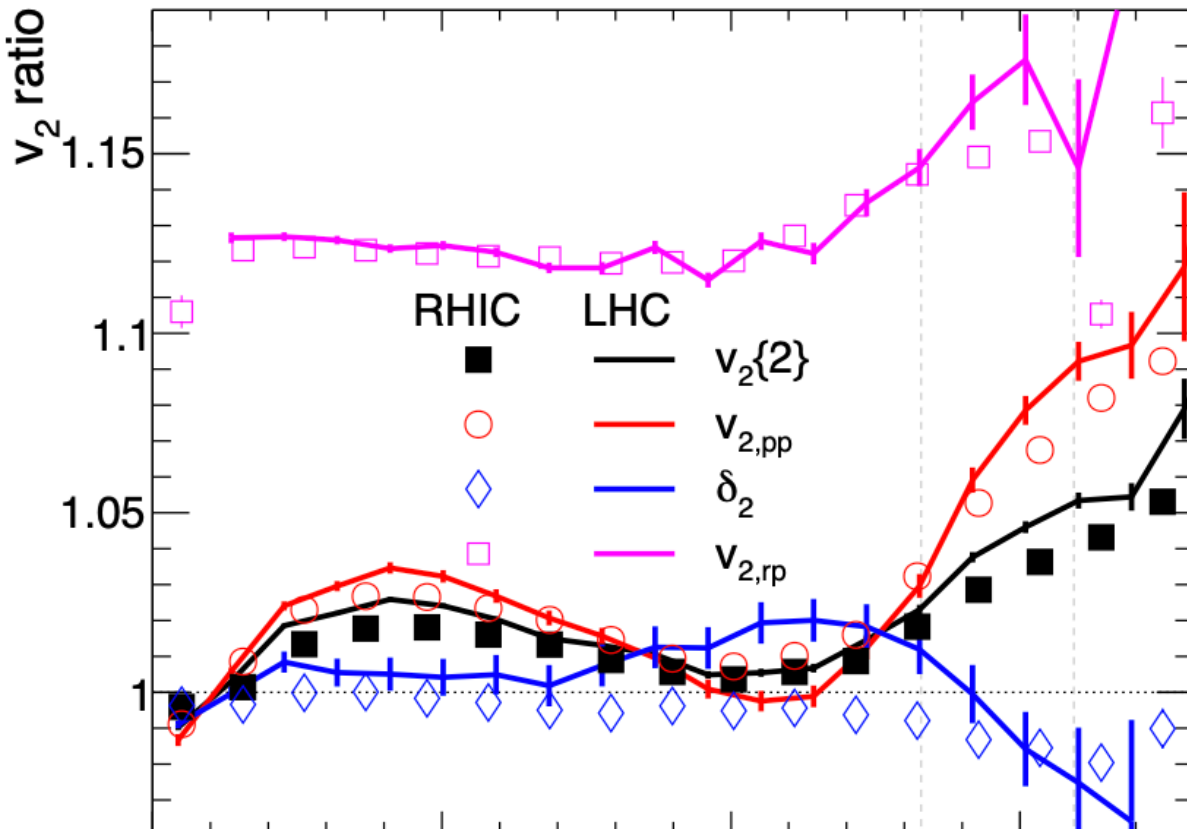


FIG. 7: The response coefficients for various definition and components of v_2 (left) and v_3 (right) at the RHIC energy.

Elliptic Flow (v_2): Observation



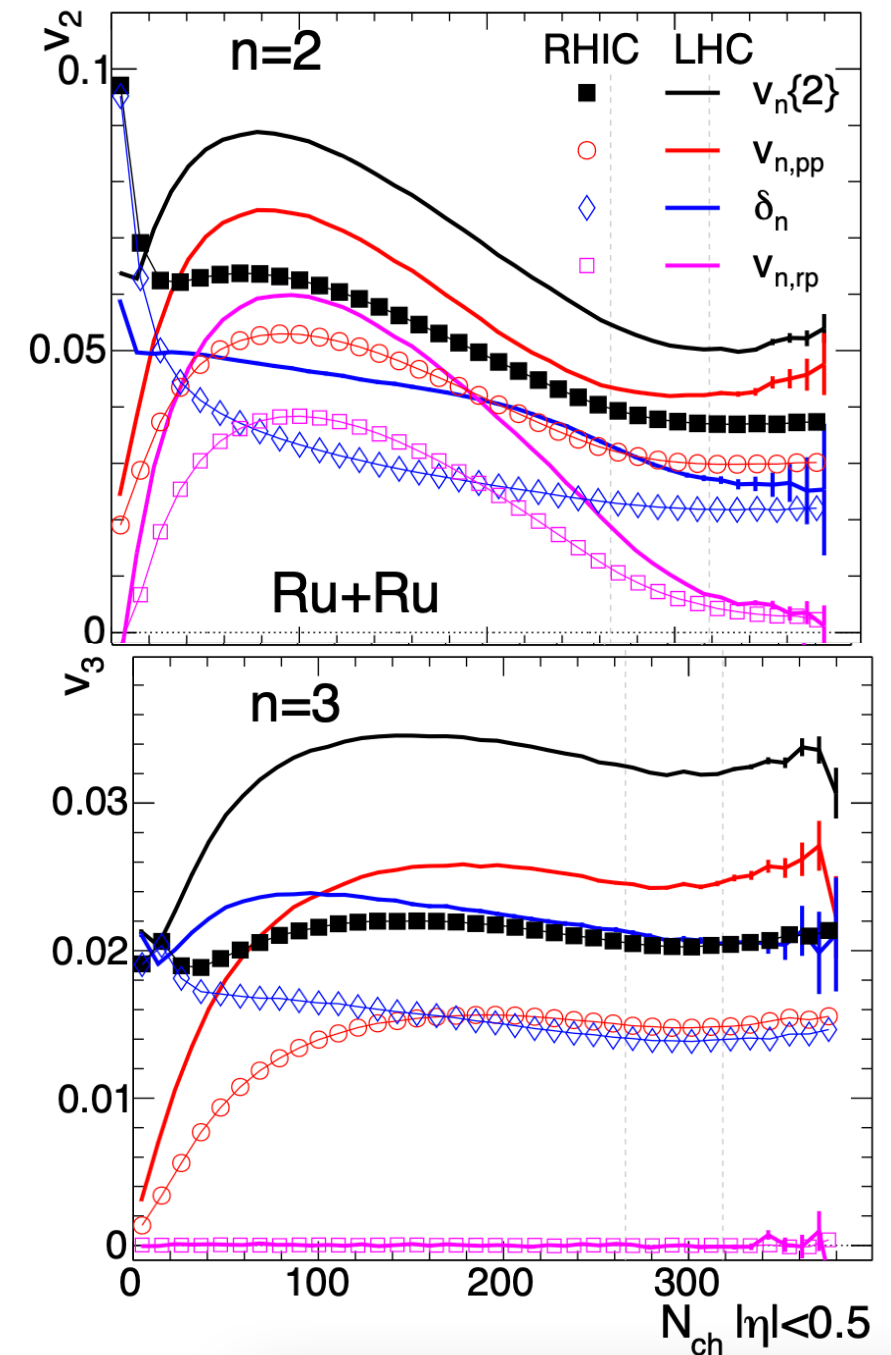
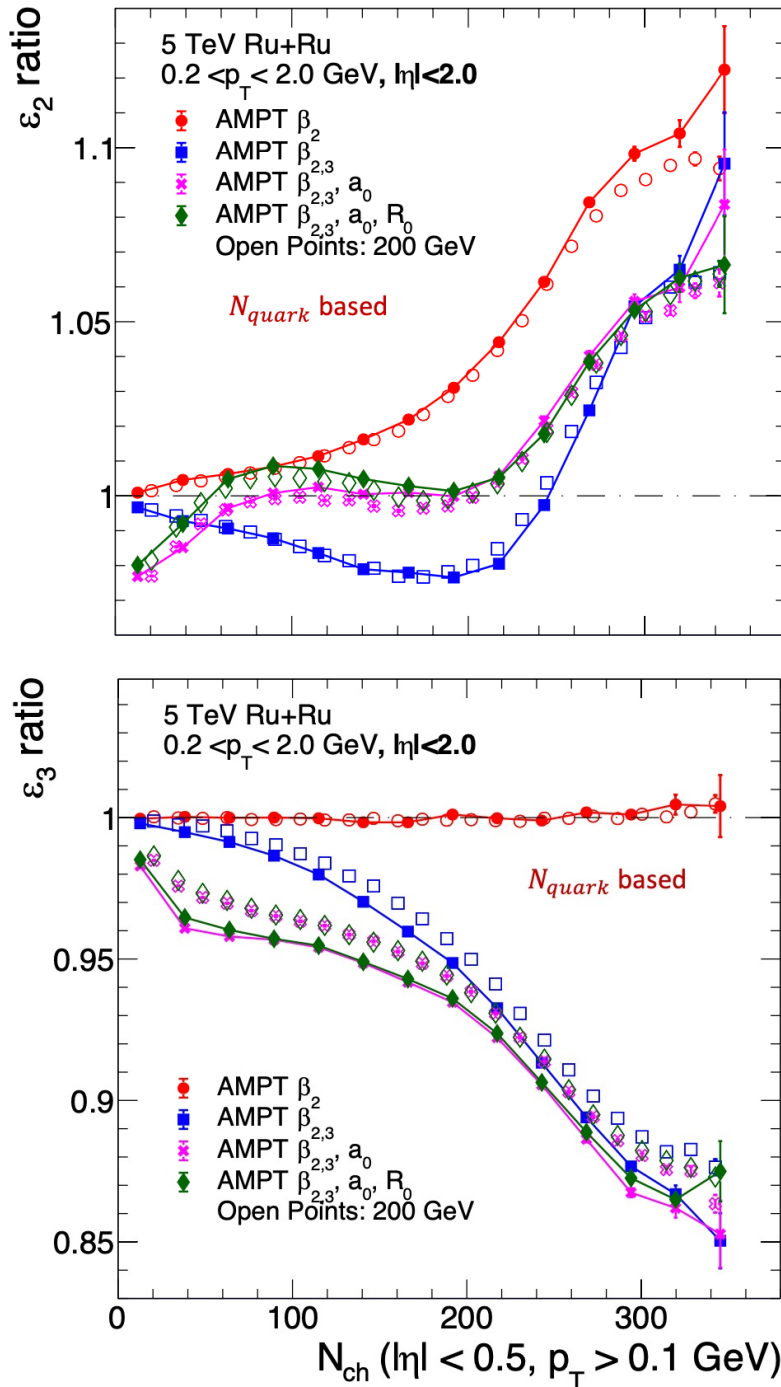
- The Ratio(v_2) have qualitative agreement between both energies for all estimates of v_2 .
- Ratio($v_{2,pp}$) $\gg 1$ due to domination of a_0 ;
- Ratio(δ_2) ~ 1 at both energies
- Ratio($v_{2,pp}$) $>$ Ratio($v_2\{2\}$).
- δ_n dilutes the effect of nuclear structure on Initial participant geometry at both energies.



➤ Structure parameters have larger contributions to v_2 ratio at LHC than at RHIC energy.

- Why is it so? Answer: Flow response coefficient

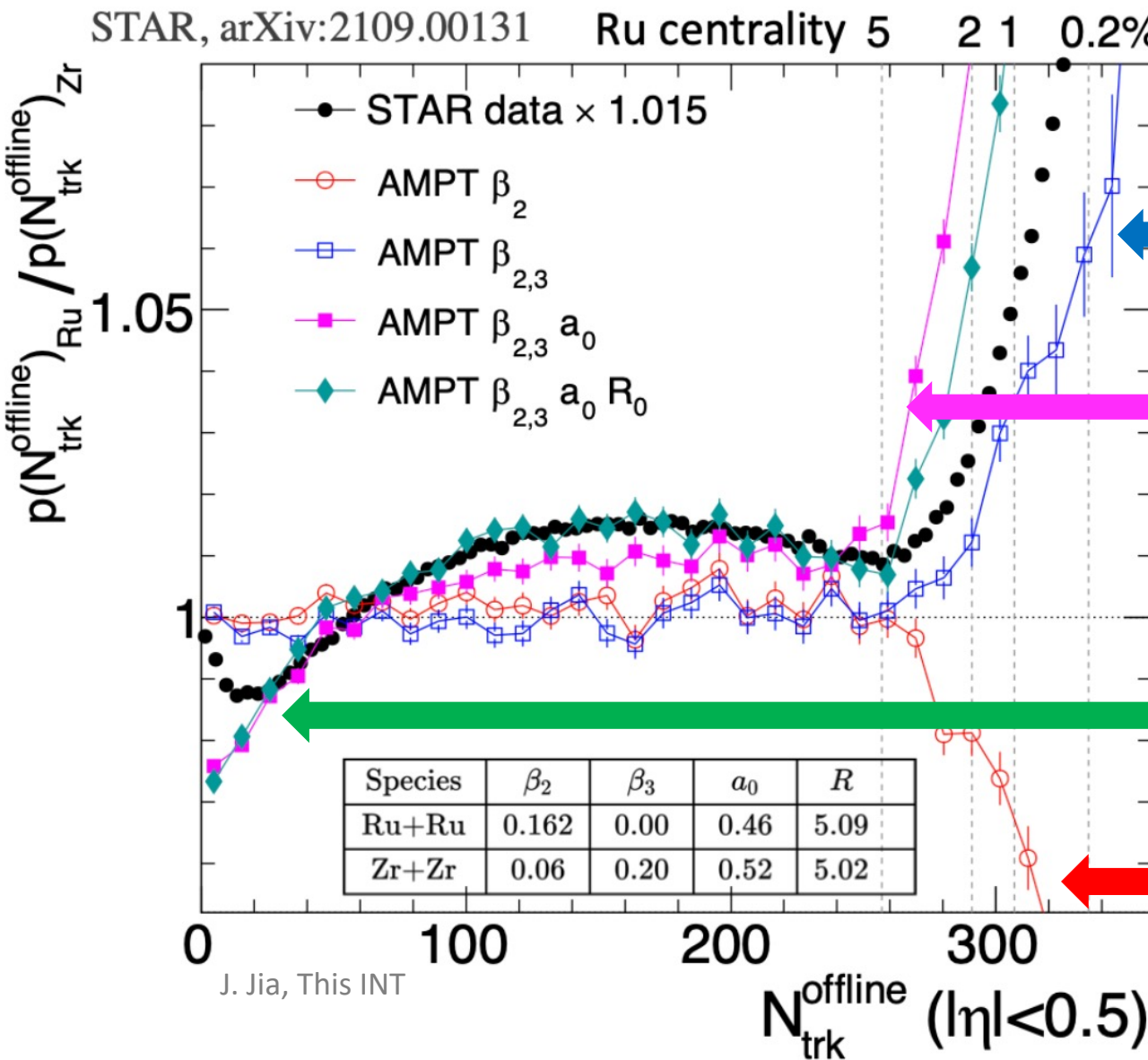
Backup



$p(N_{ch})$ ratio: RHIC

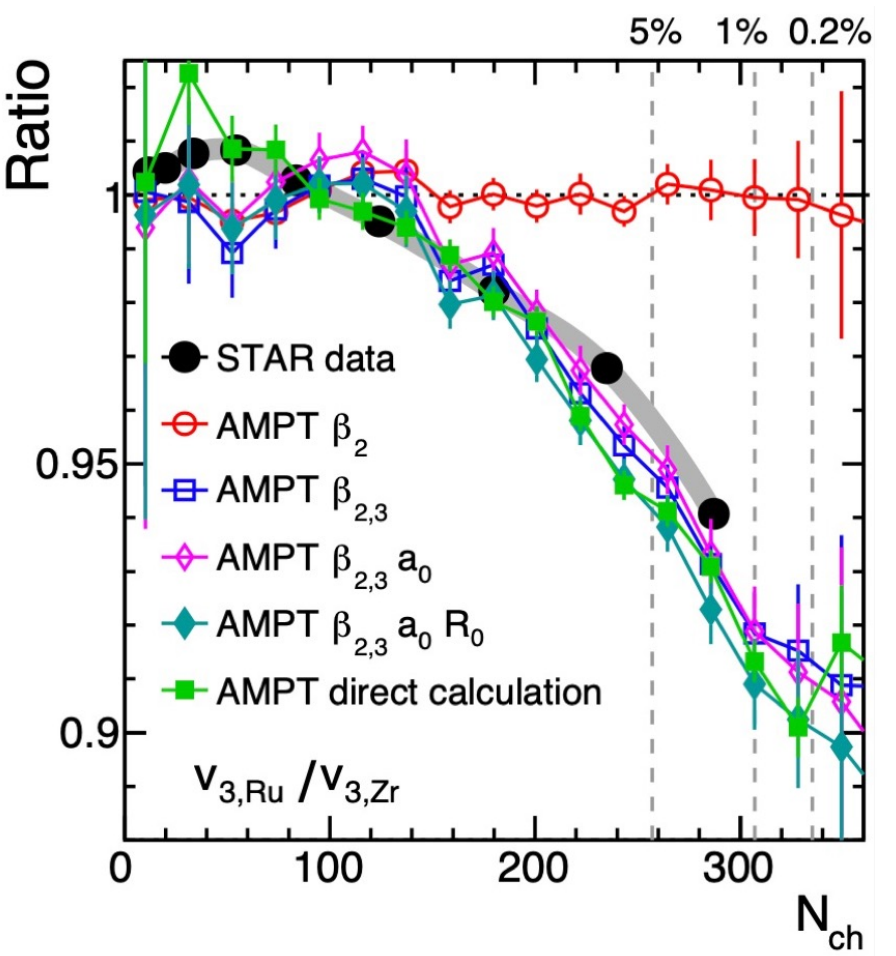
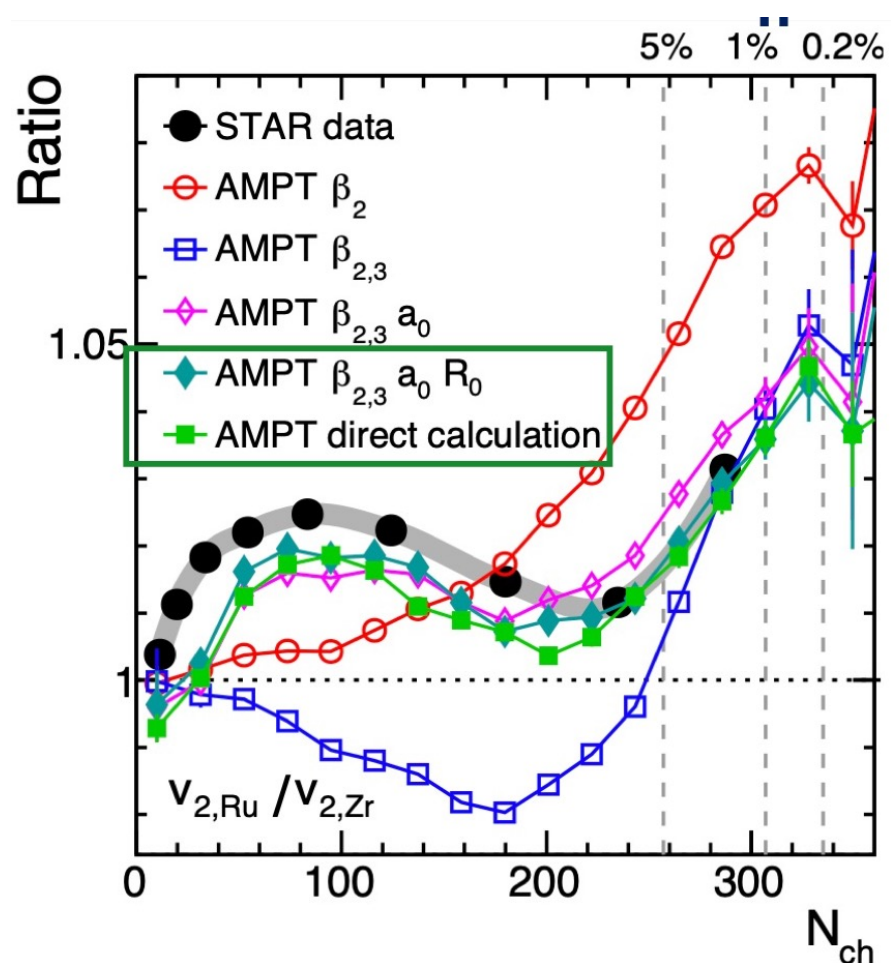
* Originates from $p(N_{part})$ in Initial stages of collision which has similar features.

| Cases | β_2 | β_3 | a_0 | R |
|-----------|-----------|-----------|-------|------|
| Ru (def.) | 0.162 | 0 | 0.46 | 5.09 |
| Case 2 | 0.06 | 0 | 0.46 | 5.09 |
| Case 3 | 0.06 | 0.2 | 0.46 | 5.09 |
| Case 4 | 0.06 | 0.2 | 0.52 | 5.09 |
| Zr | 0.06 | 0.2 | 0.52 | 5.02 |

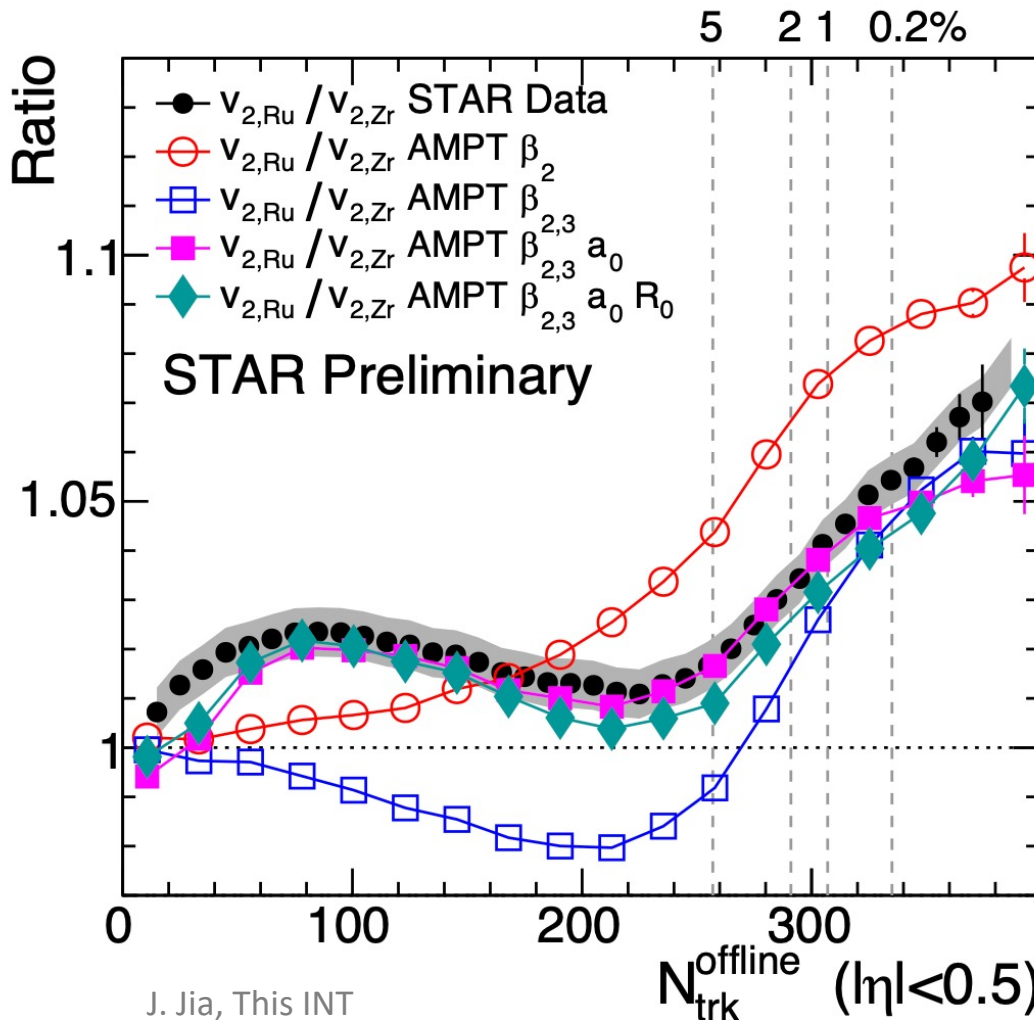


Backup

| Cases | β_2 | β_3 | a_0 | R |
|-----------|-----------|-----------|-------|------|
| Ru (def.) | 0.162 | 0 | 0.46 | 5.09 |
| Case 2 | 0.06 | 0 | 0.46 | 5.09 |
| Case 3 | 0.06 | 0.2 | 0.46 | 5.09 |
| Case 4 | 0.06 | 0.2 | 0.52 | 5.09 |
| Zr | 0.06 | 0.2 | 0.52 | 5.02 |

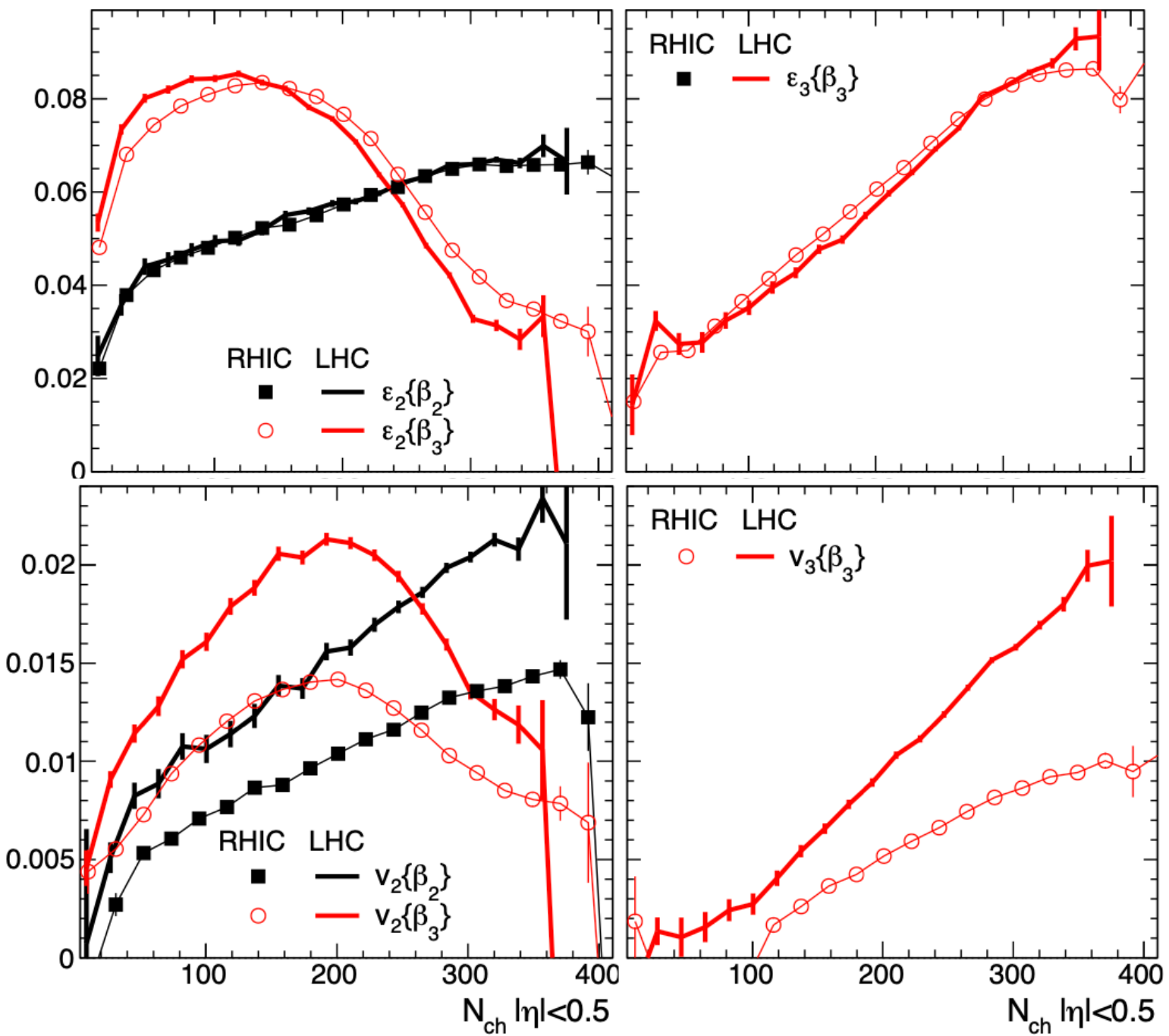


$v_2\{2\}$ ratio from RHIC

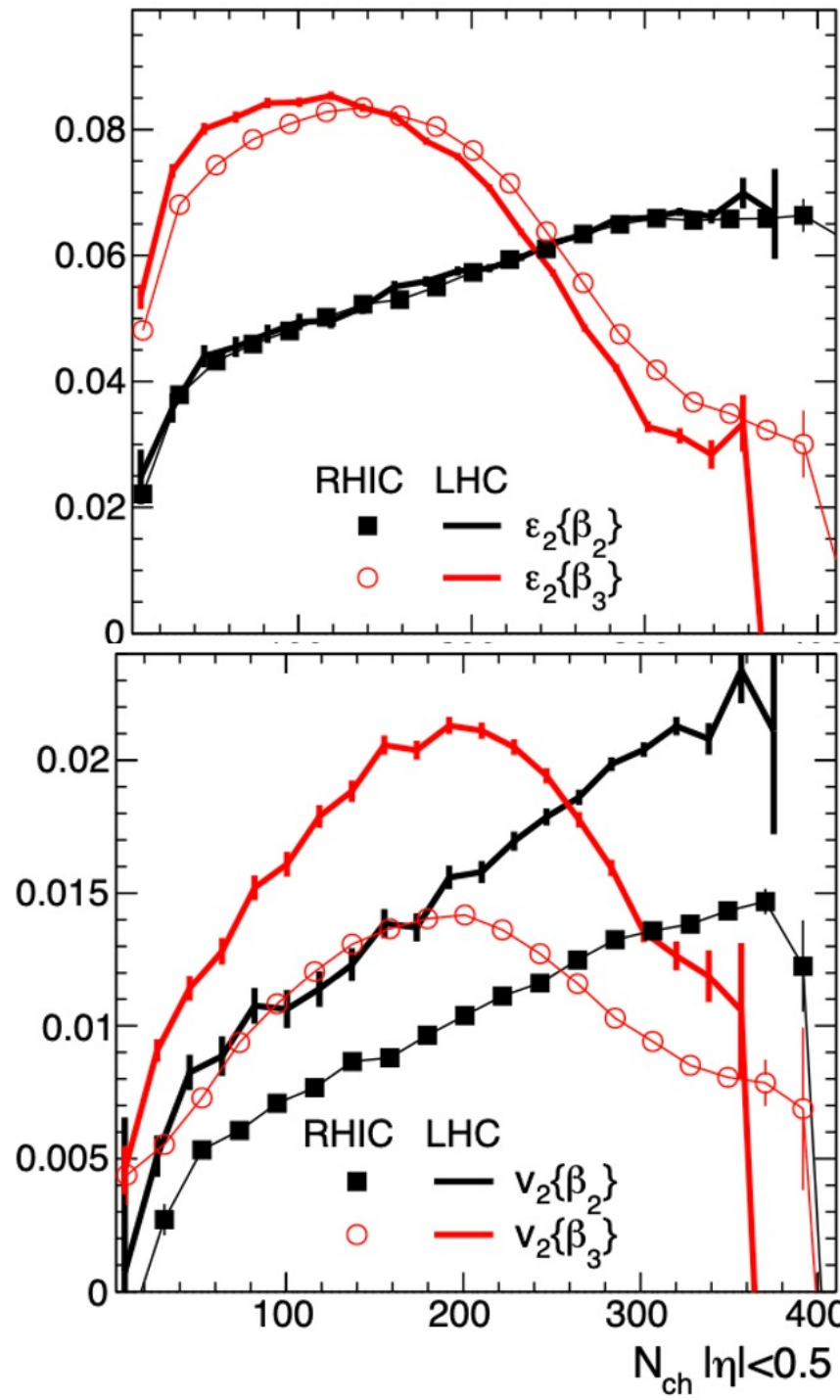
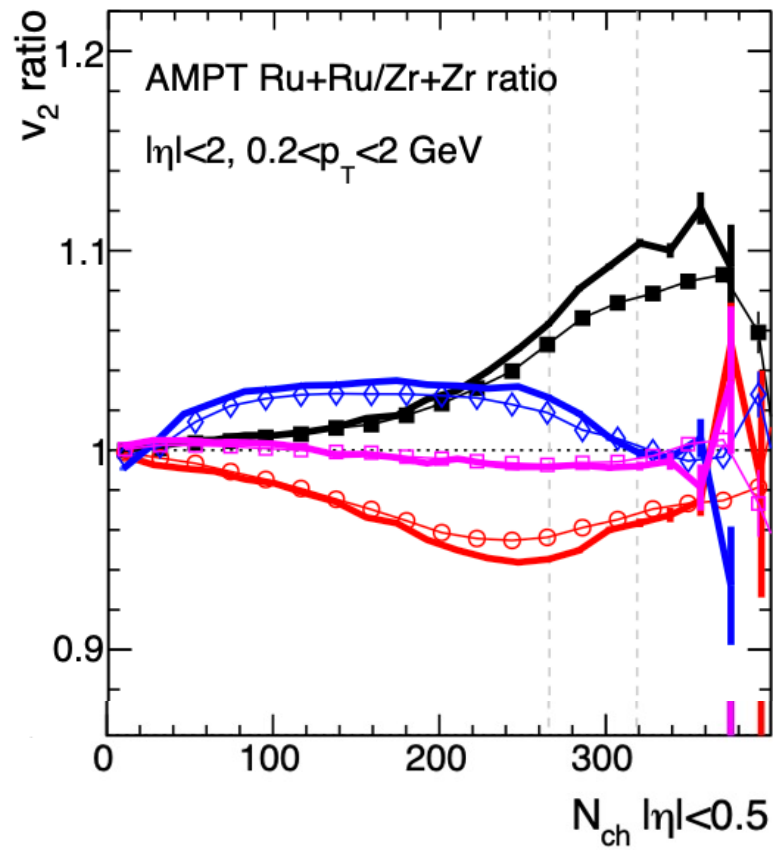


- Increasing β_2 increases v_2 , mostly in central events.
- Increasing β_3 increases v_2 , mostly in mid-central events.
- Increasing a_0 increases v_2 , in most peripheral events (limiting case).
As a consequence, in mid-central events, Increasing a_0 decreases v_2 .
- Increasing R_0 has a very small effect on v_2 in mid-central events.

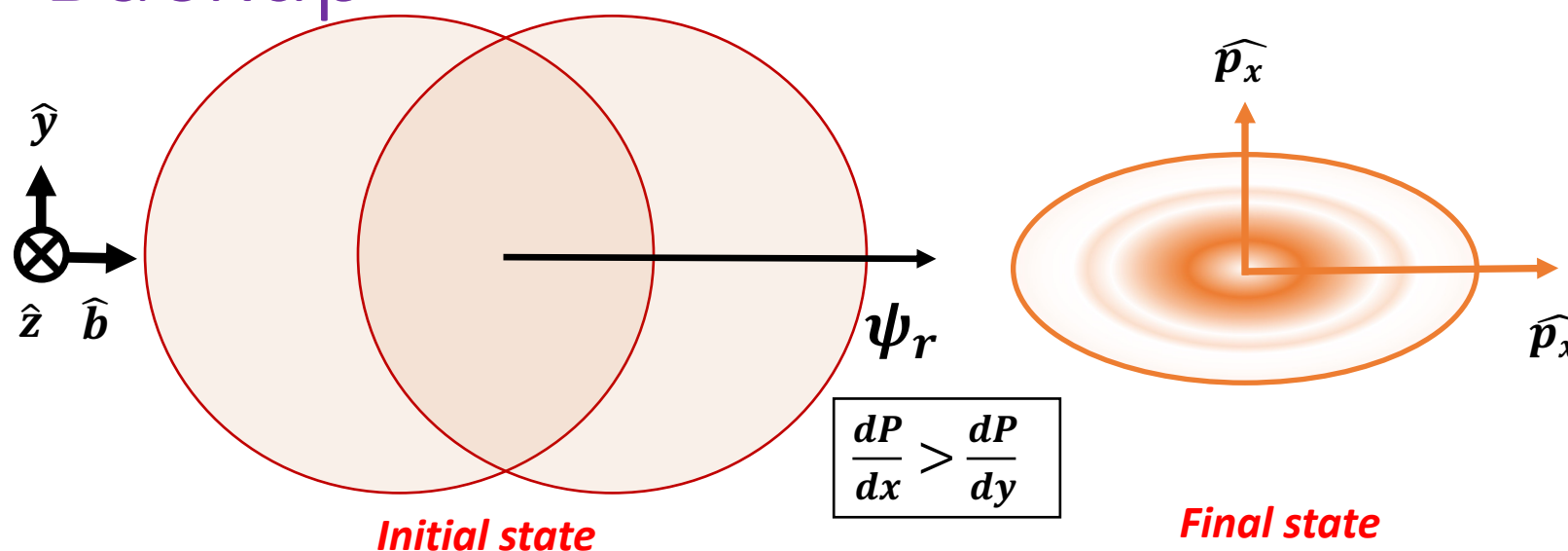
Backup



Backup

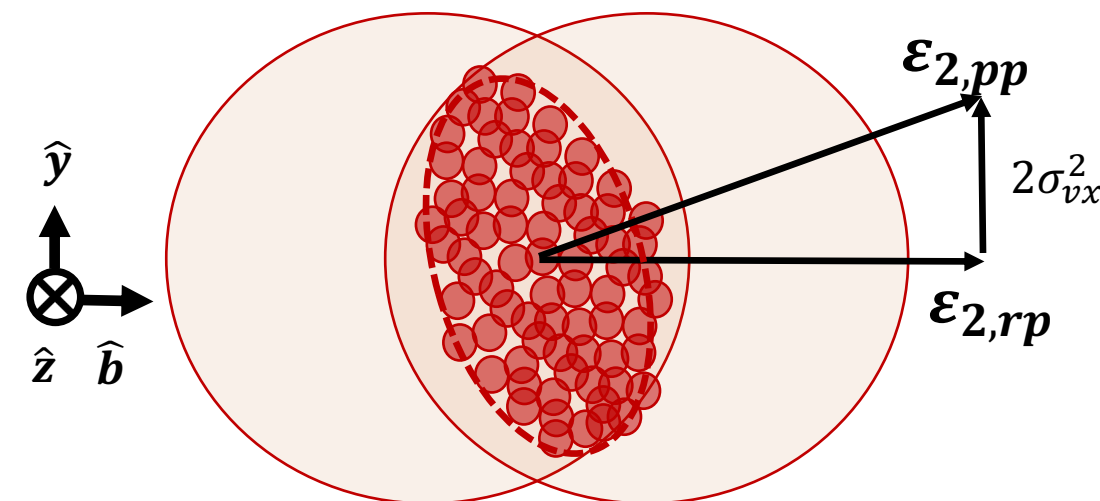


Backup

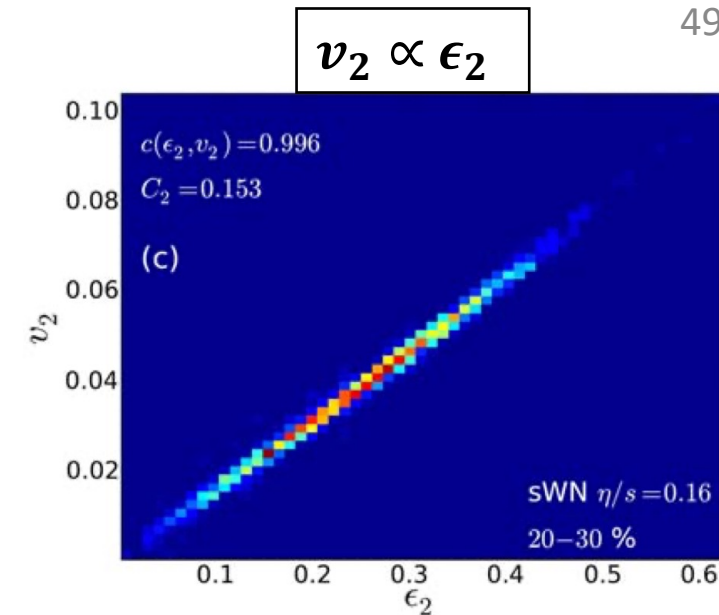


- Pressure gradients convert Initial spatial anisotropy to final state momentum anisotropy.

- Flow fluctuations play an important role in estimate of rms flow.



$$\begin{aligned}
 v_2^2\{2\} &= \langle k^2 \varepsilon_{pp}^2 \rangle + \delta_{\text{Non-Flow}} \\
 &= k^2(\langle \varepsilon_{rp}^2 \rangle + 2\sigma_{\varepsilon,x}^2) + \delta_{\text{Non-Flow}} \\
 &= \langle v_{rp}^2 \rangle + 2\sigma_{vx}^2 + \delta_{\text{Non-Flow}}
 \end{aligned}$$



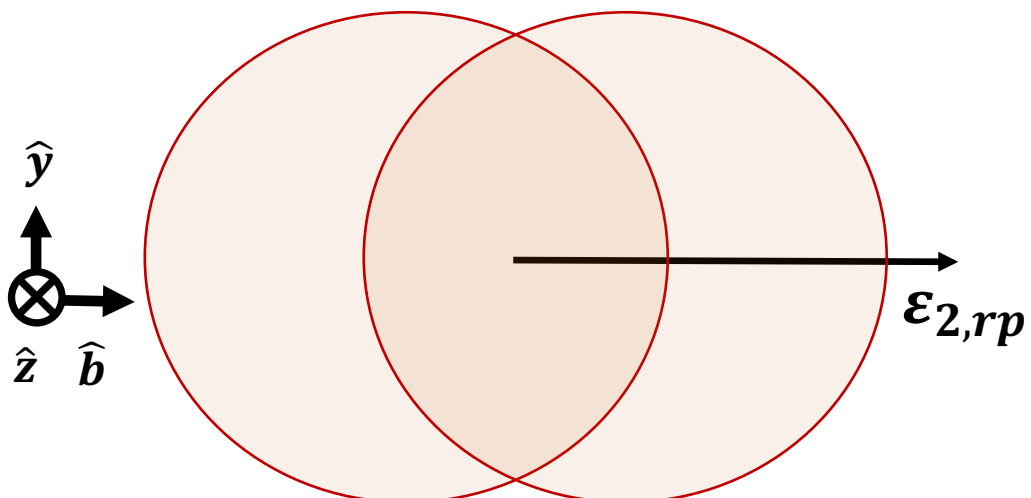
Backup

$$\begin{aligned}
 & v_2^2\{2\} \\
 &= \langle \cos 2(\phi_i - \phi_j) \rangle = \langle \cos 2(\phi_i - \Psi_{rp} + \Psi_{rp} - \phi_j) \rangle \\
 &= \langle \cos 2[(\phi_i - \Psi_{rp}) - (\phi_j - \Psi_{rp})] \rangle \\
 &= \langle \cos 2[(\phi_i - \Psi_{rp})] \cos 2[(\phi_j - \Psi_{rp})] \rangle + \langle \text{sin terms} \rangle \\
 &= \langle v_{2,rp}^2 \rangle + \text{Non-Flow correlations}
 \end{aligned}$$

$$\begin{aligned}
 & \langle v_{2,rp}^2 \rangle \\
 &= \langle v_{2,rp} \rangle^2 + (\langle v_{2,rp}^2 \rangle - \langle v_{2,rp} \rangle^2) \\
 &= \langle v_{2,rp} \rangle^2 + (\sigma_{vx}^2 + \sigma_{vy}^2) \text{(Bessel Gaussian assumption; } \vec{v}_2 = \vec{v}_{2,x} + \vec{v}_{2,y} \text{)} \\
 &= \langle v_{2,rp} \rangle^2 + 2\sigma_{vx}^2 \text{(Flow fluctuations)}
 \end{aligned}$$

$$v_2^2\{2\} = \langle \cos 2(\phi_i - \phi_j) \rangle_{evt} = \langle \cos 2(\phi_i - \Psi_{rp} + \Psi_{rp} - \phi_j) \rangle_{evt} = \langle v_{2,rp}^2 \rangle_{evt} + \delta_{Non-Flow}$$

Observable: Elliptic Flow (v_2)

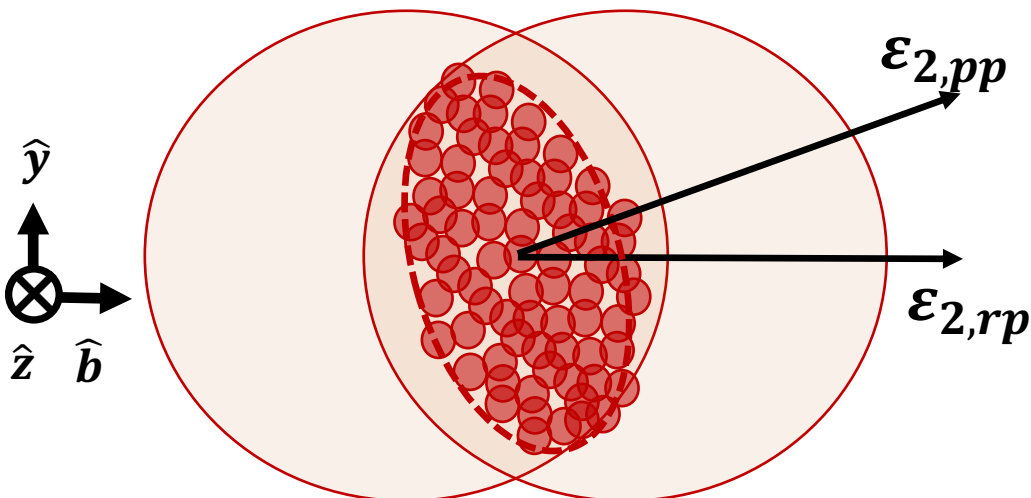


- $\varepsilon_{2,RP}$ represents eccentricity arising from average geometry.

$$\vec{\varepsilon}_{2,RP} = \left\langle \frac{\sigma_y^2 - \sigma_x^2}{\sigma_y^2 + \sigma_x^2} \right\rangle \hat{i}$$

- $v_{2,RP}$: flow arising from average geometry.

$$v_{n,RP} = \frac{|\langle V_n \varepsilon_{n,RP}^* \rangle|}{\sqrt{\langle \varepsilon_{n,RP} \varepsilon_{n,RP}^* \rangle}}$$



- $\varepsilon_{2,PP}$ represents eccentricity arising from IS fluctuations.

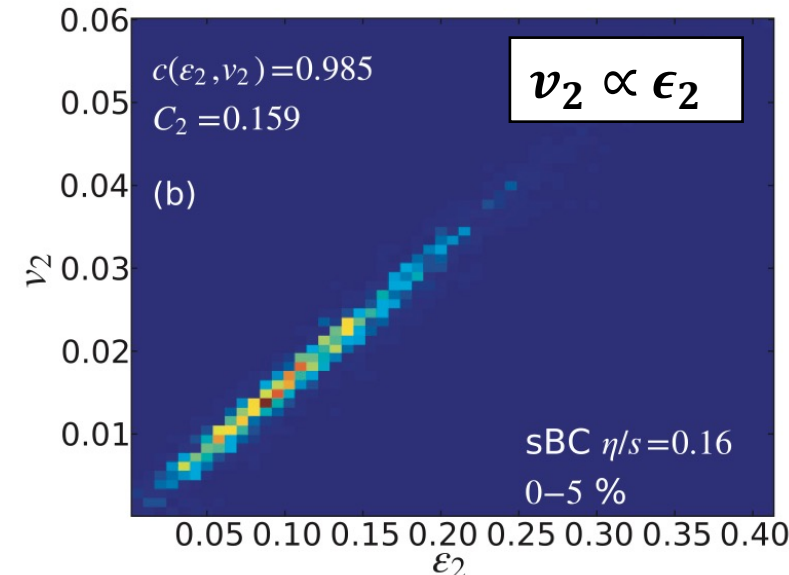
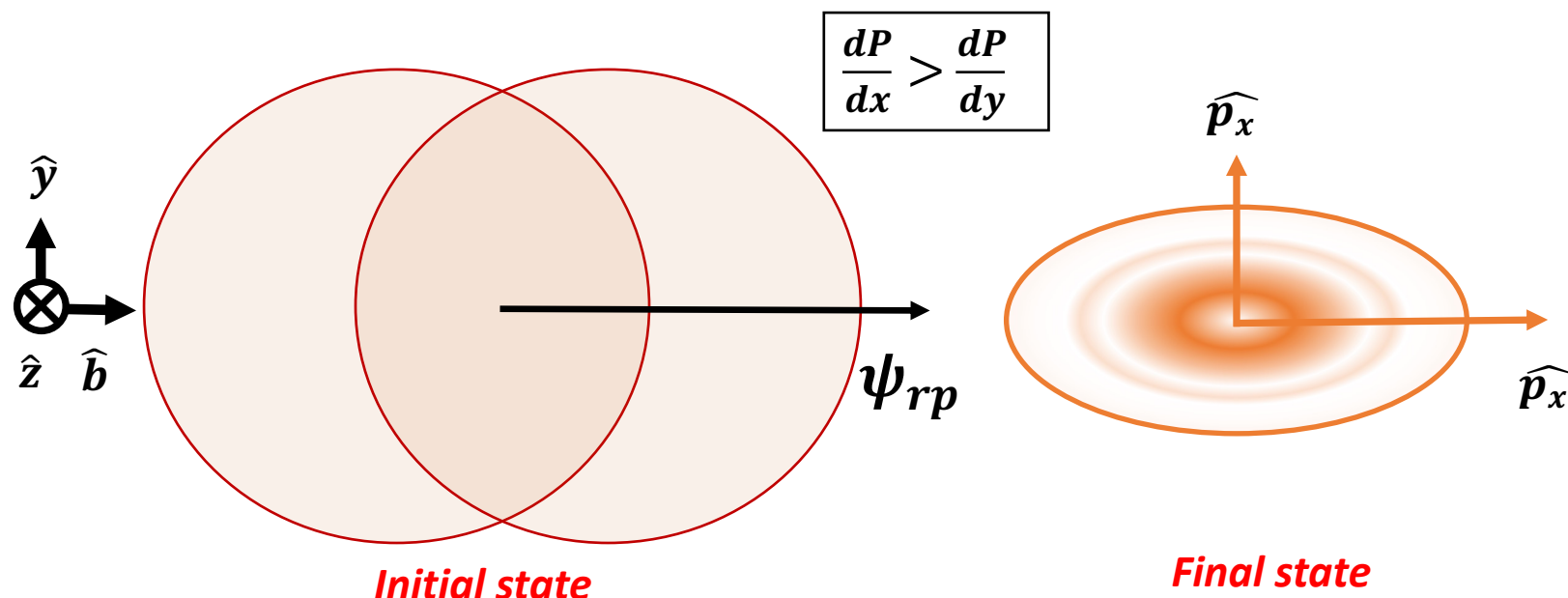
$$\vec{\varepsilon}_{2,PP} = \left\langle \frac{\sigma_y^2 - \sigma_x^2}{\sigma_y^2 + \sigma_x^2} \right\rangle \hat{i} + \left\langle \frac{2\sigma_{xy}}{\sigma_y^2 + \sigma_x^2} \right\rangle \hat{j}$$

- $v_{2,PP}$: flow arising from participant geometry in IS.

$$v_{n,PP} = \frac{\langle V_n \varepsilon_{n,PP}^* \rangle}{\sqrt{\langle \varepsilon_{n,PP} \varepsilon_{n,PP}^* \rangle}}$$

Projection of \vec{V}_n along $\vec{\varepsilon}_{n,PP}$

Observable: Elliptic Flow (v_2)



PRC.87.054901

- Pressure gradients convert Initial spatial anisotropy to final state momentum anisotropy.

$$E \frac{d^3N}{d^3p} = \frac{1}{2\pi} \frac{d^2N}{p_t dp_t dy} \left(1 + \sum_{n=1}^{\infty} 2v_n \cos(n(\varphi - \Psi_r)) \right)$$

$$v_2 = \langle \cos 2(\phi_i - \Psi_{rp}) \rangle_{evt}$$

- Many methods to estimate v_2 : 2-particle correlation $v_2\{2\}$ gives the RMS value of flow.

$$v_2^2\{2\} = \langle v_{2, rp} \rangle^2 + 2\sigma_{vx}^2 + \delta_{Non-Flow}$$